



Kaunas University of Technology
Faculty of Mechanical Engineering and Design

Development of PCB-Based Electromagnetic Actuation Drive

Master's Final Degree Project

Mažvydas Samuolis

Project author

Prof. Egidijus Dragašius

Supervisor

Kaunas, 2022



Kaunas University of Technology
Faculty of Mechanical Engineering and Design

Development of PCB-Based Electromagnetic Actuation Drive

Master's Final Degree Project
Mechatronics (6211EX017)

Mažvydas Samuolis

Project author

Prof. Egidijus Dragašius

Supervisor

Lect. Joris Vėžys

Reviewer

Kaunas, 2022



Kaunas University of Technology
Faculty of Mechanical Engineering and Design
Mažvydas Samuolis

Development of PCB-Based Electromagnetic Actuation Drive

Declaration of Academic Integrity

I confirm the following:

1. I have prepared the final degree project independently and honestly without any violations of the copyrights or other rights of others, following the provisions of the Law on Copyrights and Related Rights of the Republic of Lithuania, the Regulations on the Management and Transfer of Intellectual Property of Kaunas University of Technology (hereinafter – University) and the ethical requirements stipulated by the Code of Academic Ethics of the University;
2. All the data and research results provided in the final degree project are correct and obtained legally; none of the parts of this project are plagiarised from any printed or electronic sources; all the quotations and references provided in the text of the final degree project are indicated in the list of references;
3. I have not paid anyone any monetary funds for the final degree project or the parts thereof unless required by the law;
4. I understand that in the case of any discovery of the fact of dishonesty or violation of any rights of others, the academic penalties will be imposed on me under the procedure applied at the University; I will be expelled from the University and my final degree project can be submitted to the Office of the Ombudsperson for Academic Ethics and Procedures in the examination of a possible violation of academic ethics.

Mažvydas Samuolis
Confirmed electronically



Kaunas University of Technology

Faculty of Mechanical Engineering and Design

Task of the Master's final degree project

Given to the student – Mažvydas Samuolis

1. Title of the project

Development of PCB-Based Electromagnetic Actuation Drive

(In English)

Elektromagnetinės pavaros PCB pagrindu kūrimas

(In Lithuanian)

2. Hypothesis

A PCB-based array of flat coils can be used for multi-DoF electromagnetic actuation of millimeter-scale objects.

3. Aim and tasks of the project

Aim: To develop a universal PCB-based electromagnetic actuation drive for millimeter-scale movements.

Tasks:

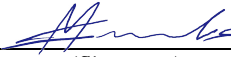
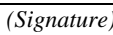
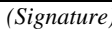
1. To design a PCB-based flat coil for repulsion of millimeter-scale permanent magnet (1-5mm).
2. To compare the designed flat coil's theoretical model and physical prototype.
3. To design proof-of-concept electromagnetic drive based on the previously designed flat coil.
4. To produce the designed drive and experimentally derive its characteristics (maximum speed, payload capacity and positioning accuracy).
5. To evaluate economic viability of the designed drive.

4. Initial data of the project

Minimum stroke of 10mm; maximum PCB stator size of 100mm by 100mm; maximum speed not less than 100mm/s; minimum payload capacity 10g; minimum positioning resolution of 0.5mm.

5. Main requirements and conditions

COMSOL Multiphysics 5.4 for FEM simulations; KiCad 6.0 for development of custom PCB and electronics schematics; any precision laboratory power supply for experiments with flat coils; any gaussmeter capable of testing magnetic flux density in 0.1mT to 10mT range; any thermal imager operational in 20°C to 150°C range.

Project author	Mažvydas Samuolis		2022-02-28
	<i>(Name, Surname)</i>	<i>(Signature)</i>	<i>(Date)</i>
Supervisor	Egidijus Dragašius		2022-02-28
	<i>(Name, Surname)</i>	<i>(Signature)</i>	<i>(Date)</i>
Head of study field programs	Regita Bendikienė		2022-02-28
	<i>(Name, Surname)</i>	<i>(Signature)</i>	<i>(Date)</i>

Mažvydas Samuolis. Development of PCB-Based Electromagnetic Actuation Drive. Master's Final Degree Project, supervisor prof. Egidijus Dragašius; Faculty of Mechanical Engineering and Design, Kaunas University of Technology.

Study field and area (study field group): Production and Manufacturing Engineering (E10), Engineering Sciences (E).

Keywords: Planar drive, PCB stator, magnetic levitation, electromagnetic drive, flat coils.

Kaunas, 2022. 53 p.

Summary

This project presents a proof-of-concept multi-degree-of-freedom electromagnetic planar drive with a PCB-based stator and an untethered permanent magnet mover. Utilizing a PCB-based stator allows to develop easily customizable, low mechanical complexity, and affordable systems for the use in robotic assembly operations, precision micromachining, precision positioning and manipulation, as well as cleanroom manufacturing and material handling.

This work proposes a PCB-based stator topology comprising 2D array of flat electromagnetic coils. In order to achieve this, firstly a FEM analysis of individual flat coils is carried out, selecting two best performing coils for physical tests – both with 0.1mm track width and spacing, 0.035mm copper layer thickness, 4mm in diameter; one single-layer, another two-layer. Then, a physical PCB testbed, consisting of 4 distinct test zones (individual coil test zone, linear motion test zone, rotary motion test zone, and planar motion test zone) is developed and manufactured. Using this testbed, experiments are firstly performed on the individual coils, demonstrating a maximum magnetic flux density of 0.6mT for the single-layer coil and 0.9mT for the double-layer coil, which is in agreement with the FEM results. Next, the experiments demonstrated that both double and single-layer coils have a maximum payload capacity of approximately 1.5g for pulsed current and approximately 1g for continuous current (considering specific thermal dissipation setup used for the tests). Lastly, the 3 developed stators with a basic control algorithm allowed to demonstrate 101mm/s linear speed, and 125rpm rotational speed. Further work on a custom motor driver is advised to reach the maximum potential of the developed drives with PCB-based stators.

Finally, economic viability of a custom multi-DOF electromagnetic planar drive with a PCB-based stator is evaluated. With assumptions that 3 full-time engineers are employed in order to maintain and further develop the product to customer specifications, as well as 20-unit demand of custom drives a year, the value of one full system with a 30% profit margin totals 6721€.

Mažvydas Samuolis. Elektromagnetinės pavaros PCB pagrindu kūrimas. Magistro baigiamasis projektas, vadovas prof. Egidijus Dragašius; Kauno technologijos universitetas, Mechanikos inžinerijos ir dizaino fakultetas.

Studijų kryptis ir sritis (studijų krypčių grupė): Gamybos inžinerija (E10), Inžinerijos mokslai (E).

Reikšminiai žodžiai: Plokštuminė pavara, PCB statorius, magnetinė levitacija, elektromagnetinė pavara, plokščiosios ritės.

Kaunas, 2022. 53 p.

Santrauka

Magistro baigiamasis projektas pristato kelių laisvės laipsnių elektromagnetinės plokštuminės pavaros, su fiziškai neprijungta judančia dalimi bei PCB pagrindu sukurtu statoriumi, koncepciją. PCB pagrindu kuriamas statorius suteikia galimybę projektuoti lengvai pritaikomas, nesudėtingos mechanikos bei prieinamos kainos sistemas, kurios gali būti panaudojamos robotinio surinkimo operacijoms, mikro-apdirbimui, tikslaus pozicionavimo ir valdymo sistemoms, bei gamybinėms operacijoms švarios patalpos aplinkoje.

Šiame darbe pristatoma PCB pagrindu sukurta statoriaus topologija yra sudaryta iš plokščiųjų elektromagnetinių ričių 2D masyvo. Jai sukurti, pirmiausia, BEM būdu buvo analizuojamos pavienės plokščiosios ritės, taip atrenkant dvi tinkamiausias rites praktiniams testams – abi su 0.1 mm takelio bei tarpelio pločiu, 0.035 mm vario sluoksnio storiu, 4 mm diametro; pirmoji vieno sluoksnio, antroji – dviejų. Tada buvo suprojektuota ir pagaminta fizinė bandomoji PCB plokštė, sudaryta iš 4 skirtingų dalių: pavienių ričių testavimo zona; linijinės pavaros statoriaus testavimo zona; sukimo pavaros statoriaus testavimo zona; plokštuminės pavaros testavimo statoriaus zona. Pirmiausia, pasitelkiant bandomąją plokštę, buvo ištestuotos pavienės ritės: pademonstruotas didžiausias magnetinio srauto tankis lygus 0.6 mT vieno sluoksnio ritei ir 0.9 mT dviejų sluoksnių ritei – tai patvirtino BEM simuliacijų rezultatus. Papildomi eksperimentai nustatyti maksimaliai apkrovai parodė, kad abi ritės gali atlaikyti po 1.5 g laikiną apkrovą ir 1 g nuolatinę apkrovą (su šiais testams naudota specifine šilumos išsklaidymo struktūra). Galiausiai, buvo pritaikyti nesudėtingi judesio valdymo algoritmai, kurie su šiais statoriais leido pasiekti 101 mm/s linijinį greitį bei 125 rpm sukimosi greitį. Didesnis greitis ir geresnis valdymas galėtų būti pasiekti su papildomai suprojektuotu variklio valdikliu.

Paskutiniame projekto etape buvo apskaičiuoti keli ekonominiai indikatoriai PCB pagrindu sukurtai pavarai įvertinti. Darant prielaidą, kad šiam produktui techniškai palaikyti ir toliau tobulinti reikėtų 3 inžinierių, numatant 20 sistemų metinius pardavimus, vienos pilnos sistemos kaina su 30 % marža siektų 6721 €.

Table of contents

List of figures	8
List of tables	10
Introduction	11
1. Relevance and Novelty of Research	13
1.1. Relevance of Research	13
1.2. Novelty of Research	14
2. Literature Review	17
2.1. Overview of Electromagnetic Coil Array Stator Topologies	17
2.1.1. Planar MDOF Electromagnetic Actuator Stator Based on Several MMLM.....	17
2.1.2. Planar Electromagnetic Actuator Based on Stator-Long 1D Conductor Assemblies	18
2.1.3. Planar Electromagnetic Actuator Based on 2D Coil Array Design	19
3. Practical Considerations for PCB-Based Stator	22
3.1. PCB Manufacturing.....	22
3.2. Electromagnetic Analysis of PCB-Based Flat Coils	23
4. Development of PCB-Based Electromagnetic Drive Stator	27
4.1. Modelling of a Single Flat Coil	27
4.1.1. FEM-Based Electromagnetic Analysis of PCB Flat Coils	27
4.2. PCB-Based Stator Testbed Development.....	30
5. Experiments With PCB-Based Stators for an Electromagnetic Drive	34
5.1. Experiments With Individual Coils	34
5.2. Experiments With Generating Linear and Rotary Motion	38
5.3. Experiments With Generating 2D Planar Motion	41
6. Discussion	43
7. Economic Viability of Custom Planar Drive With PCB-Based Stator	45
7.1. Costs	45
7.2. Pricing.....	46
Conclusions	48
List of references	50

List of figures

Fig. 1. Milli-scale parallel assembly robotic system developed by researchers Liu and Ravindra, comprising: a) aluminum stator; b) electromagnets; d) robots with permanent magnets and tweezers [3]	13
Fig. 2. PCB-based magnetically actuated drives used in: a) axial flux motors [6]; b) automated 2D micro-assembly [11]; c) nanoliter fluid handling [10]; d) fluidic injection system [13].....	14
Fig. 3. Stator-long conductors topology proposed by Ueda and Ohsaki [14]	15
Fig. 4. 2D coil arrays for electromagnetic planar drive: herringbone pattern (left), round coil 2D array (middle), electrodynamic planar motor (right) [15]	16
Fig. 5. Topology of a moving magnet actuator based on 4 MMLM proposed by Zhu et al. [1]	17
Fig. 6. Planar actuator's topology based on 3 MMLM proposed by Schaffel er al. [16].....	18
Fig. 7. PCB-based serpentine traces for planar electromagnetic actuator's stator [4]	18
Fig. 8. Electromagnetic planar drive concept proposed by Lu and Usman [17].....	19
Fig. 9. A) Herringbone pattern; b) electrodynamic planar drive; c) 2D array of round coils [15]....	20
Fig. 10. Standard composition of a multi-layer PCB [24]	22
Fig. 11. Micro electromagnetic coils analyzed by Majlis et al. [29]: a) parallel planar circular coil; b) spiral planar circular coil	24
Fig. 12. Structure of MEMS actuator using PCB micro-coil developed by Majlis et al. [29]	24
Fig. 13. Flat coils for inductive sensing by Meydan et al. [30].....	25
Fig. 14. Coil topologies of new PCB coil actuators by Carl Bugeja [31]	25
Fig. 15. Maximum magnetic flux density reached by the flat coils designed by Carl Bugeja [31]..	26
Fig. 16. Comparison of achieved magnetic flux density by different configurations of flat coils [31]	26
Fig. 17. A single coil to be used in FEM simulations - 12mm outer coil diameter, 0.07mm copper layer thickness, and 0.2 mm track width and spacing on a 1.6mm thickness PCB.....	28
Fig. 18. FEM simulation results for different coil configurations with the highest magnetic flux density, showing its distribution around each coil: 12mm OD, 7.7mT & 165°C (top left), 12mm OD, 8.15mT & 222°C (top right), 12mm OD 5.8mT & 139°C (middle left), 4mm OD, 8.7mT & 211°C (middle right) and 4mm OD, 7mT & 58°C (bottom)	29
Fig. 19. Simulated thermal performance of a PCB-based flat coil with varying parameters: a) maximum temperature of 165°C with 12mm OD on 1 layer (0.07mm CT); b) 211°C with 6mm OD on 2 layers (0.035mm CT); c) 84°C with 4mm OD on 2 layers (0.035mm CT).	30
Fig. 20. PCB view of stators testbed: two separate flat coils (top), linear drive stator configuration (left), rotary drive stator configuration (bottom), and planar drive stator configuration (middle)....	31
Fig. 21. Schematic view of electronics setup applicable to linear, rotary, and planar drives configurations	32
Fig. 22. a) 4 magnets for individual flat coil tests; b) two movers with selected type of magnet (nr. 3), one for planar motion testing (left) and one for rotary motion testing (right)	33
Fig. 23. A testbed of stators developed for PCB-based electromagnetic drive experiments	34
Fig. 24. Current to payload relation for single-layer (top) and double-layer (bottom) coils with 4 different magnets	35
Fig. 25. Main equipment used for the experiments: a) <i>LongWei PS3010DF</i> precision laboratory power supply [37]; b) <i>Proster VC99</i> multimeter [34]; c) <i>Seek Shot</i> thermal imaging camera [35]; d) <i>Lakeshore Model 475 DSP</i> gaussmeter [36]	36

Fig. 26. Individual coil thermal tests: a) 1-layer coil at 0.5A; b) 2-layer coil at 0.5A; c) 2-layer coil at 0.5A with a heatsink; d) 1-layer coil at 1.1A; e) heatsink; f) the two individual coils with heatsink on the backside	36
Fig. 27. Magnetic flux density test setup: a) hall effect probe with exact sensor location [36]; b) testbed with probe taking a measurement; c) Gaussmeter showing nearly maximum measurement of 2-layer coil at 0.5A	37
Fig. 28. Setup for payload tests: a) precision electronic scale; b) nuts used as masses; c) payload test for 1-layer coil supporting 1.5g; d) payload test for 2-layer coil supporting 1.25g	38
Fig. 29. PCB testbed of stators prepared for the linear motion tests	39
Fig. 30. Starting code for all three configurations tests – linear, rotary, and planar	39
Fig. 31. Code for: a) basic linear motion of 60mm forward and backward; b) around a 30mm diameter circle	40
Fig. 32. Screen captures of a video demonstrating 100mm/s linear motion, starting at image a)	40
Fig. 33. Screen captures of a video demonstrating 120rpm rotary motion, starting at image a)	41
Fig. 34. Screen captures of a video demonstrating planar motion around the perimeter of 4-by-4 coil grid.....	41
Fig. 35. Code for looping planar motion around the perimeter of the 4-by-4 coil grid	42
Fig. 36. FEM simulation result of a single-layer coil for magnetic flux density between 0.6mT and 1.6mT.....	44

List of tables

Table 1. Summary of 3 most common moving magnet actuator's stator topologies	21
Table 2. Comparison of three widely used PCB manufacturers, performed in November of 2021 .	23
Table 3. Summary of PCB-coil modelling results using FEM, at 0.5A input current.....	28
Table 4. Experimentally obtained resistance, temperature and magnetic flux measured for individual coils.....	34
Table 5. Capital investment related costs, as well as a summary of fixed and variable costs	45

Introduction

Multi-degree-of-freedom (multi-DOF) electromagnetic actuators based on magnetic levitation have demonstrated great potential in recent years, both for researchers, and for industrial applications as well. With untethered mover (or in specific cases rotor) and multi-DOF motion, they offer to replace more conventional multi-DOF systems with several single-DOF drives connected in series, or other, more intricate devices based on micro-electromechanical system (MEMS) drives. It is mostly due to such advantages as non-contact parallel multi-DOF motion capability, a potential for unlimited stroke with high precision, a compact system design, its modularity and potential for customization. In fact, these novel maglev drives have already found applications in robotic assembly operations, precision micromachining, haptic interaction, precision positioning and manipulation, as well as cleanroom manufacturing and material handling.

While the untethered movers of planar electromagnetic drives are application-specific and predominantly consisting of permanent magnet arrays, stators have only 3 prevalent topologies. They can be composed of a 2D array of electromagnets, they can be based on stator-long 1D conductor assemblies, or they can be made up of several moving magnet linear motors working in parallel to provide multi-DOF planar motion. These are often complicated and expensive multi-part systems, requiring high precision manufacturing and assembly operations. Recently, however, due to improvements in printed circuit board (PCB) manufacturing technology, it became possible to simplify electromagnetic planar drive stator design for small-payload, high-precision systems by designing stators with all conductors based fully on a PCB.

In fact, stator topology based on stator-long 1D conductor assemblies have already been successfully implemented on a PCB by several researchers. Moreover, PCB-based flat electromagnetic coils have also been employed as miniature 1D actuators for various purposes. However, no research has been found on the electromagnetic planar drive stators based on the other two topologies, where the stator is fully PCB-based. Furthermore, as the topology based on 2D array of coils has been shown to have the greatest power efficiency of the three, as well as excellent controllability, it is particularly suitable for a small-scale, low-payload planar drive with PCB-based stator. Consequently, this project aims to show that a PCB-based array of flat coils can be used for multi-DoF electromagnetic actuation of millimeter-scale objects.

It is achieved through firstly analyzing variations of isolated flat electromagnetic coils with the help of finite element modelling (FEM) software. Once the best performing variation is found, it is used to develop a PCB testbed with 4 distinct test zones: one for experiments with an isolated coil, one for linear drive's stator, one for rotary drive's stator, and final one for planar drive's stator. The first zone is used for experiments to compare the developed flat coil's theoretical performance with its factual performance, including its payload capacity, thermal characteristics, and magnetic flux density. The other 3 test zones are then utilized to demonstrate the maximum linear and rotary speed achievable with such a prototype, as well as to show potential for using this stator topology for a planar electromagnetic drive.

Finally, economic viability of a planar drive based on a 2D array of flat coils is evaluated. This task is completed assuming that the research subject of this work is fully developed into a working product, which could then be of interest to a range of university researchers and R&D companies in need of

more affordable high-precision customizable miniature 6 DOF actuators, capable of operating in cleanroom environments.

Aim:

To develop a universal PCB-based electromagnetic actuation drive for millimeter-scale movements.

Tasks:

1. To design a PCB-based flat coil for repulsion of millimeter-scale permanent magnet (1-5mm).
2. To compare the designed flat coil's theoretical model and physical prototype.
3. To design proof-of-concept electromagnetic drive based on the previously designed flat coil.
4. To produce the designed drive and experimentally derive its characteristics (maximum speed, payload capacity and positioning accuracy).
5. To evaluate economic viability of the designed drive.

1. Relevance and Novelty of Research

1.1. Relevance of Research

Recently, modular, configurable, and small footprint motion systems have been receiving more interest across various disciplines and industries. In particular, researchers have been looking at novel electromagnetic drives to be employed in semiconductor, flat panel display, and optics manufacturing, where vacuum or cleanroom environment is necessary [1]; in mechanical micromachining, where high precision is of particular importance [2]; in micro to milli-scale parallel assembly operations (Fig. 1) [3, 4]; to replace standard radial flux drives with smaller footprint, higher torque and power density axial flux electromagnetic drives [5, 6]. And even though the electromagnetic motion systems have been around for decades, it is still possible to improve upon them, especially mechanically, by miniaturizing them, simplifying structurally and making them more affordable.

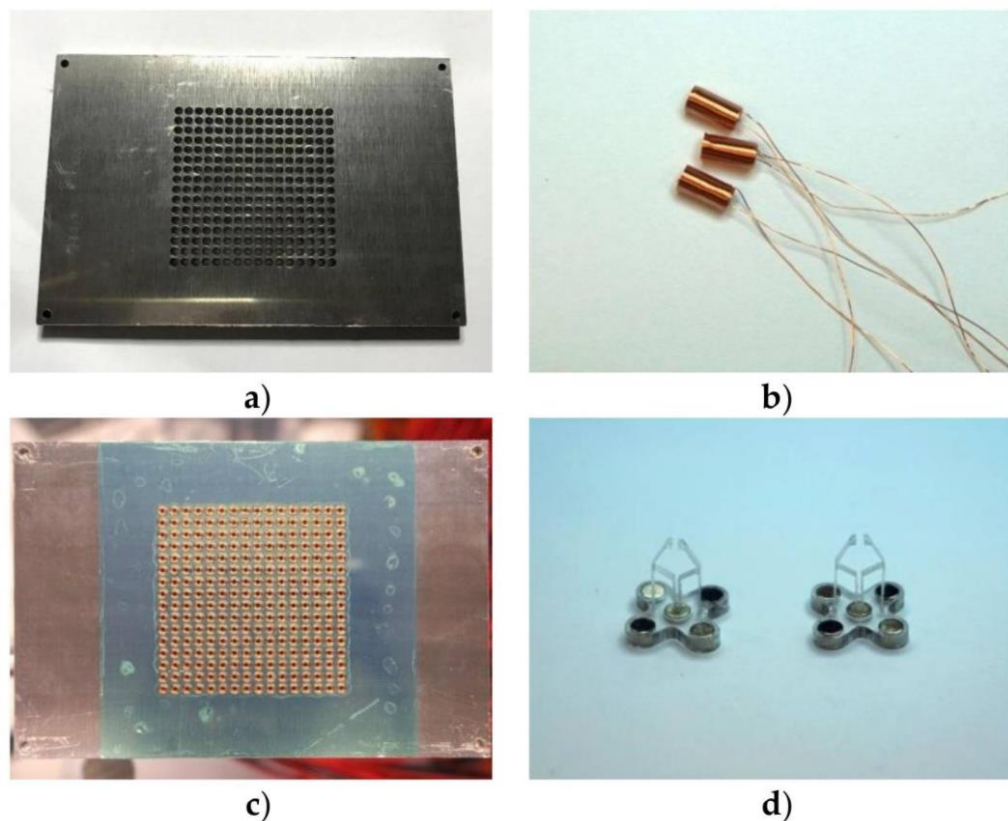


Fig. 1. Milli-scale parallel assembly robotic system developed by researchers Liu and Ravindra, comprising: a) aluminum stator; b) electromagnets; d) robots with permanent magnets and tweezers [3]

In general, magnetic actuation-based systems can offer advantages such as a potential for multidirectional and unlimited stroke, as well as untethered mover [7], and excellent thermal characteristics due to static electromagnetic field generating conductors. Moreover, planar electromagnetic actuation drives can be very compact, as it is possible to have parallel control for all degrees of freedom, in contrast to serial control with multiple stacked drives; no limitations in the amount of movers, their form factor, or the direction of movement, with upside down and vertical movement also possible [8]; more straightforward control owing to reduced system complexity arising from backlash and friction in standard electromagnetic drives.

Recently, in an effort to reduce manufacturing complexity, to make magnetic actuation systems more affordable and easier to customize, researchers have been looking at PCB-based electromagnetic coils. Particular attention has been given to rotary drives with PCB-based stators (Fig. 2, image a). It is mostly due to the potential to significantly reduce the size and weight of the motors, while reducing manufacturing costs and increasing drive efficiency [5, 6, 9]. Researchers have also demonstrated interest in PCB stators for magnetically actuated parallel milli-scale robots used in parallel assembly and micro-factory, and lab-on-chip applications (Fig. 2, images b, c and d) [4, 10–13]. In this case, PCB-stator offers multi-degree-of-freedom motion control in a single PCB package, greatly simplified manufacturing and assembly of the system, independent control of multiple movers, and modular construction.

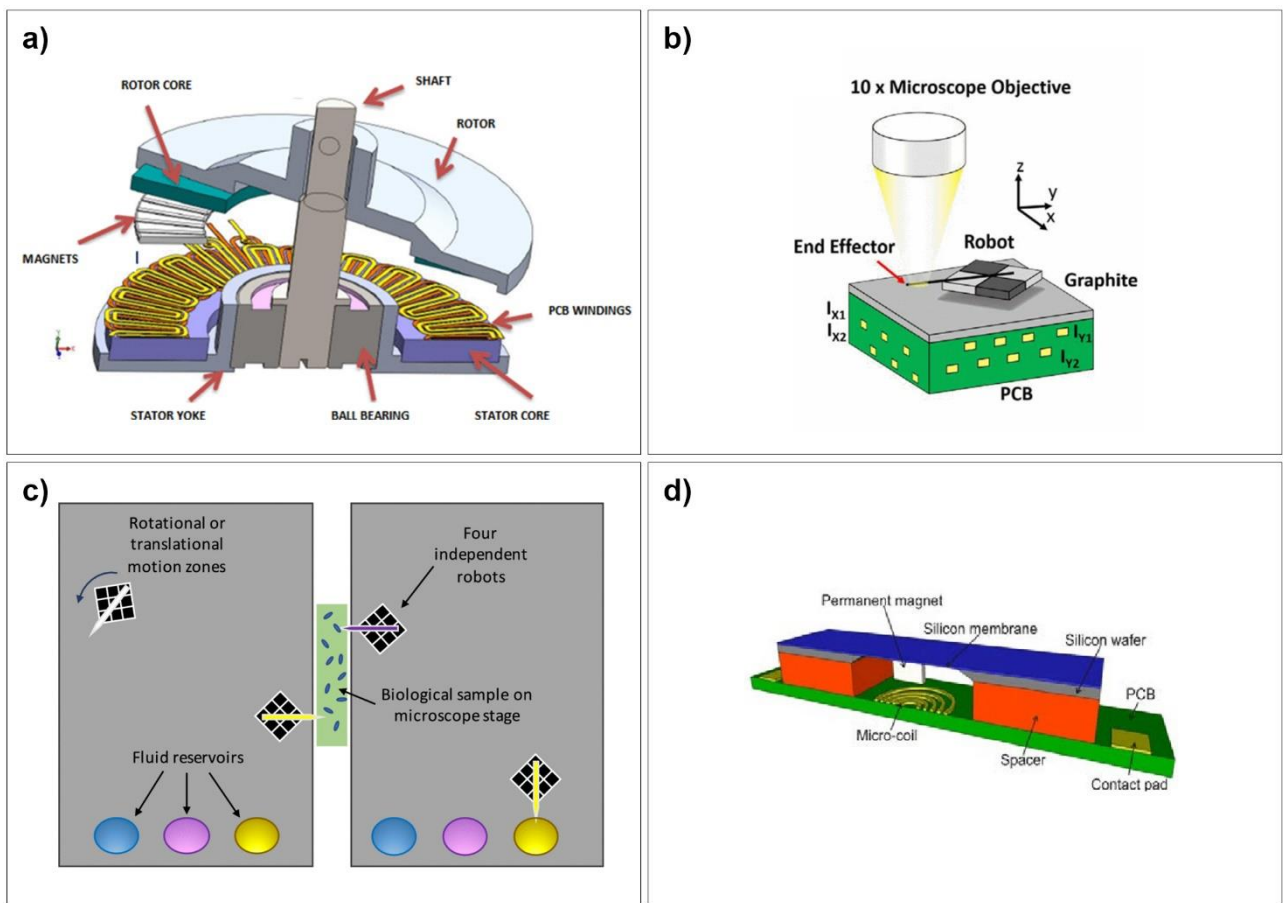


Fig. 2. PCB-based magnetically actuated drives used in: a) axial flux motors [6]; b) automated 2D micro-assembly [11]; c) nanoliter fluid handling [10]; d) fluidic injection system [13]

1.2. Novelty of Research

There is ongoing research into electromagnetic actuation-based drives in an effort to increase efficiency and power density, to make drives more affordable and easier to customize, to make them smaller and easier to manufacture. As a result, researchers are studying electromagnetic drives both with physically wound coils, and more recently with PCB-based electromagnetic coils. When it comes to more complex cases of more than 1 degree-of-freedom electromagnetic actuation, there is often no one-size-fits-all solution. It is mostly because of each application having its own

requirements, such as number of degrees of freedom, stroke length, system size, payload capacity, level of precision, and cost, as universally best physical system design does not usually exist. Moreover, there exists a level of complexity when combining physical system design with a suitable control strategy, which leaves space for improvement of system responsiveness, power efficiency, or how the system deals with force ripples and external disturbances.

One popular electromagnetic drive topology recently analysed by a number of different researchers is for magnetically actuated planar drives where the stator is fully PCB-based, composed of stator-long 1D conductor tracks (Fig. 3) [4, 10–13]. This system configuration allows for a simple and minimal mechanical construction, which is capable of achieving 6 degrees-of-freedom motion. Furthermore, it is very modular and easy to scale, as the conductors can be extended in either direction, with no extra complexity added to the system. While it is very straightforward and easy to scale, it has some drawbacks too, such as lower efficiency and extra heating across the stator’s length and width, due to energized stator coils where no mover is present.

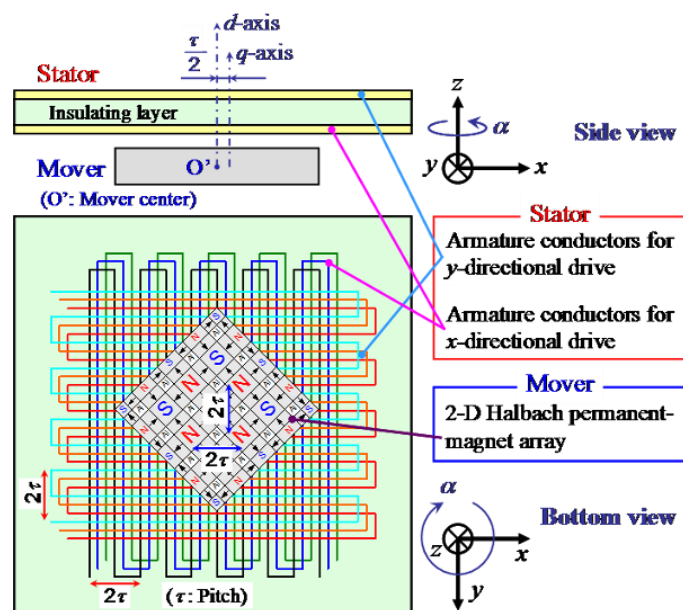


Fig. 3. Stator-long conductors topology proposed by Ueda and Ohsaki [14]

Another approach to creating electromagnetically actuated planar drives is through employing 2D coil arrays (Fig. 1 and Fig. 4). This topology is rather complex, needing numerous coils distributed throughout the full plane of the stator. Consequently, it makes the mechanical system design much more complicated, requiring a lot of different parts, including multiple electromagnetic coils and dedicated drivers. Moreover, while it is highly modular and extendible, the number of coils needed increases linearly with increasing axis length of the stator. However, this topology is very power efficient in comparison to other candidates, as it allows to have minimal number of coils active with highly concentrated magnetic fields. Additionally, it has the advantage of high precision and linearity, with accurate system force and torque models, albeit high complexity ones [15]. Consequently, there has been a lot of interest shown by researchers in studying variations of 2D coil array topologies and their various properties.

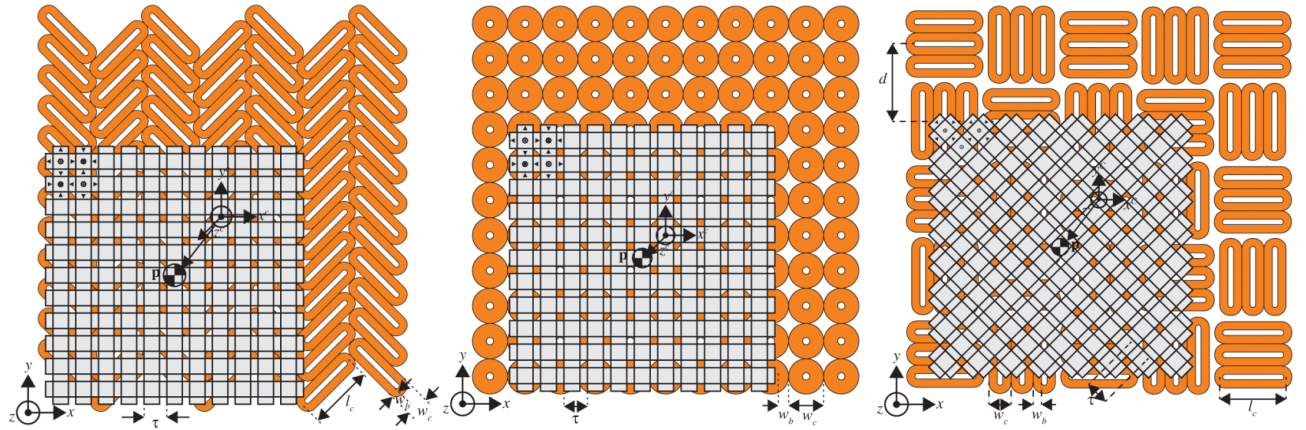


Fig. 4. 2D coil arrays for electromagnetic planar drive: herringbone pattern (left), round coil 2D array (middle), electrodynamic planar motor (right) [15]

While 2D coil array is mechanically complex when wound physically, its manufacturing and assembly operations could be greatly simplified (or nearly eliminated) if done on a printed circuit board instead. Which is why through this work an attempt was made to develop a single PCB-based flat electromagnetic coil, which could then be used as a template for a variety of electromagnetic drives with arrays of the said coil. Furthermore, universal electronics set-up and basic control strategy was developed and tested on a linear drive made up of 1D array of coils, on a rotary drive made up of the same coils patterned in a circle, as well as on a planar drive using 2D coil array.

This type of customizable drive with untethered mover could be employed in building parallel assembly cells, micro-factories, lab-on-chip cells, or miniature rotary and linear drives. Moreover, PCB manufacturing technology allows for cheap, high accuracy micro-scale features, as well as offers flexible boards, high temperature boards, and even all-metal PCBs. The combination of a simple and cheap manufacturing technique with customizable electromagnet array arrangement shows promise to simplify research into multi-DoF electromagnetic drives and greatly expands potential application areas for such actuators.

2. Literature Review

This chapter of the thesis focuses on overviewing written research papers on the topics of flat electromagnetic drives. It also concentrates on the research methods employed by the scientists in developing similar types of work. Following the review of works by other researchers, a research framework for the development of a PCB-based electromagnetic drive is formulated and followed through subsequent chapters of the thesis.

Firstly, however, it is important to discuss the key steps to be taken in the development of the electromagnetic drive. In order to have a functioning prototype, 3 equally important parts need to be considered - mechanics, electronics and control. Although all of these parts are very important in the drive to be developed, the thesis is focused primarily on the mechanical part. In particular, most of the analysis and research work is concerned with the development of a PCB-based stator for the electromagnetic drive. Before going into the methods for analysis, modelling and simulation of the electromagnetic properties of moving magnet actuator systems, the next subchapter firstly overviews the most common actuator's stator designs and their characteristics.

2.1. Overview of Electromagnetic Coil Array Stator Topologies

2.1.1. Planar MDOF Electromagnetic Actuator Stator Based on Several MMLM

To start with, the simplest method to develop an electromagnetic drive with multi-degree-of-freedom (MDOF) motion capabilities is by the use of a few moving magnet linear motors (MMLM) combined in parallel. Such a combination makes a low complexity mechanical system, simultaneously providing a way to construct a straightforward mathematical model, which can then be used for controlling levitation and propulsion of the mover. However, with MDOF system built using multiple MMLM there are some drawbacks, such as lack of system modularity or extendibility, as well as a very limited range of motion.

For example, Zhu et al. [1] designed a magnetic levitation actuator comprising 4 identical 2 degree-of-freedom linear actuators (Fig. 5). This type of moving magnet actuator system provides 6 DOF

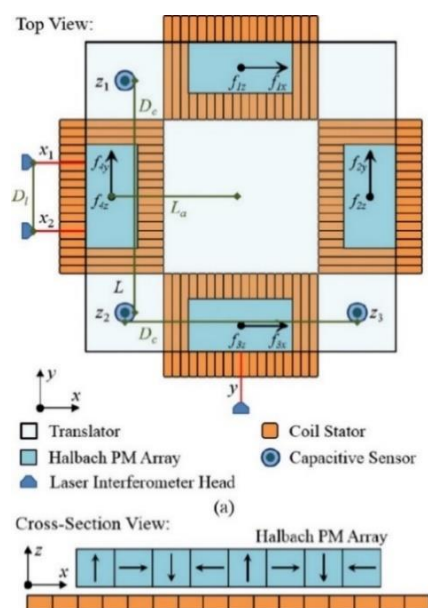


Fig. 5. Topology of a moving magnet actuator based on 4 MMLM proposed by Zhu et al. [1]

capability with both torque and force components. Every individual actuator within the stator has an array of 3-phase coils composed of 30 units of 88-turn rectangular coils (130 by 4 by 6.67mm), allowing to generate levitation, as well as simultaneous propulsion with every separate actuator. The designed electromagnetic levitation drive offers 50mm stroke both in X and Y axes, with an additional 4mm stroke along Z axis, with maximum static position error of only 200nm.

One more design based on multiple moving magnet linear actuators was proposed by Schaffel et al. [16]. In contrast to the previous system, this design requires only 3 MMLM to produce 6 degree-of-freedom motion. As a result, this system has lower mechanical complexity and reduced power requirements due to reduced number of mover parts and its lower mass. Moreover, this design comprises of only two vertically wound coils (Fig. 6), instead of multiple horizontally wound presented in the previous case. These coils generate both propelling and lifting forces by working together on a PM array mover above. The proposed actuator has 100mm stroke in X and Y axes, as well as additional 100 μ m stroke (with nanometer resolution) vertically. Lastly, motion range and payload, although both limited, they are easily scalable by altering the permanent magnet mover or coil arrays below them.

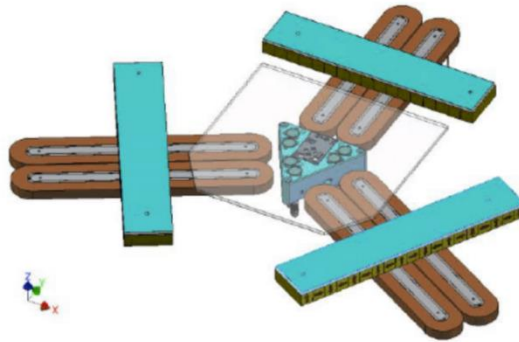


Fig. 6. Planar actuator's topology based on 3 MMLM proposed by Schaffel et al. [16]

2.1.2. Planar Electromagnetic Actuator Based on Stator-Long 1D Conductor Assemblies

One more approach to planar electromagnetic actuator's stator design is through depositing stator-long conductor assemblies (Fig. 7). This way, 6 DOF motion can also be achieved with minimal number of coils. Furthermore, this system can have virtually unlimited stroke through extending the

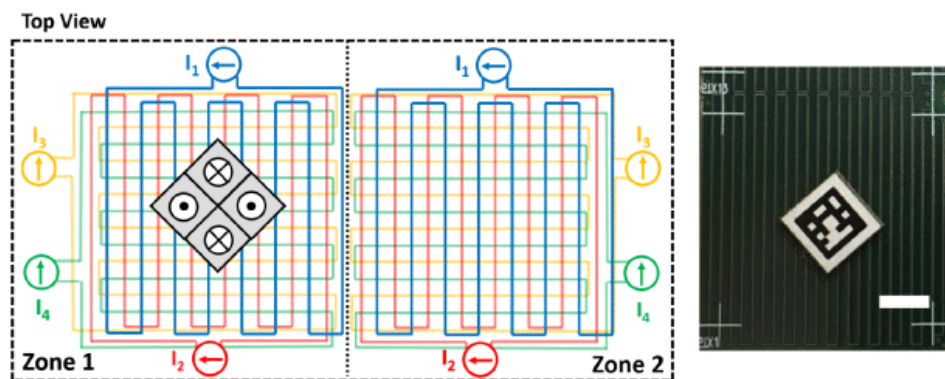


Fig. 7. PCB-based serpentine traces for planar electromagnetic actuator's stator [4]

conductors up to the desired length, both on X and Y axes, without any extra components. On the one hand, this kind of system is easily scalable and has low mechanical complexity. On the other – power efficiency is very low, and heating is present throughout the stator due to energized stator-long conductors, even without the presence of the mover.

As an example of the stator-long conductor assembly stator design, two research works were overviewed. Firstly, a PCB-based design by Lu and Usman [17], where PCB stator has 8 layers of tracks dedicated to X axis, and 8 layers of tracks to Y axis, was analyzed. This combination provides 6 DOF capability for a PM mover, as each set of coils can produce both vertical, and 1D horizontal forces. In total, however, with a mover consisting of 4 sets of Halbach arrays, the design can produce a total of 8 forces, with each individual mover segment producing separate force components for propulsion and levitation (Fig. 8). While this PCB-based actuator stator topology can provide unlimited, easily configurable motion range, with inherently eliminated coil end-effects, it produces very limited forces due to small number of turns. Additionally, this electromagnetic drive design suffers from low power efficiency, as the stator is energized throughout, despite no presence of the mover.

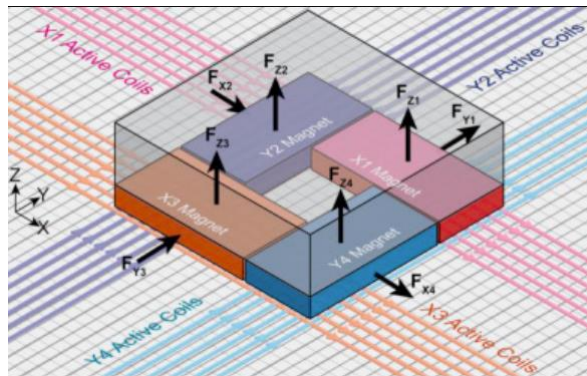


Fig. 8. Electromagnetic planar drive concept proposed by Lu and Usman [17]

In another paper, Gloess and Goos [18] demonstrated a more thorough proposal for a PCB-based stator-long conductor assembly topology design, using nearly identical structure as the one by Lu and Usman. The work presents a nanometer resolution drive with 6 DOF motion capabilities. It comprises 144 coils on a 24-layer PCB, where multiple coils can be activated independently from one another, which results in a more power efficient design. However, within the stator researchers integrated low-cost sensors with nanometer resolution, which made the control problem more difficult due to gaps between stator coils, reducing linearity and efficiency of the system.

2.1.3. Planar Electromagnetic Actuator Based on 2D Coil Array Design

The last planar electromagnetic drive stator topology to be overviewed consists of a 2D array of electromagnetic coils. This design is more challenging mechanically, electronically and control-wise, as it comprises multiple electromagnetic coils throughout the stator, needing them to work together to create continuous controllable motion. However, it is very modular, straightforward to extend it in any direction or increase its payload, but it requires twice more coils and drivers whenever an axis length is doubled. Nevertheless, it has better power-efficiency than both of the previously described topologies, as well as higher payload capacity. And while the system model is complex, the overall

system has very predictable force and torque, good linearity and precision [19]. Consequently, researchers have been exploring a multitude of 2D coil array variations for planar electromagnetic drive's stator.

For instance, Rovers et al. [20] provides a detailed comparison of three common 2D array topologies: an electrodynamic planar drive topology, a 2D array of round coils, a herringbone pattern (Fig. 9). The herringbone pattern array employing rectangular coils is distributed in such a way that X and Y axes are decoupled, with coils on each diagonal providing perpendicular horizontal forces, as well as an upwards lifting force. This stator coil array has a good fill factor, and it is the most power-efficient of all three. The round coil array design (discussed in more depth by Liu et al. [21]) is capable of providing forces in all three axes, depending on the mover's position with respect to the array. Simultaneously, however, in some positions there are coils that do not generate any useful force, making this design the least power-efficient of all three. In the final topology, each 3-phase coil set serves as an independent forcer in one horizontal axis, as well as producing a lifting force, much like in the section 2.1.1 discussed combinations of MMLMs. Although more straightforward in its distribution than the herringbone pattern, it has lower coil-fill factor, which results in higher power dissipation.

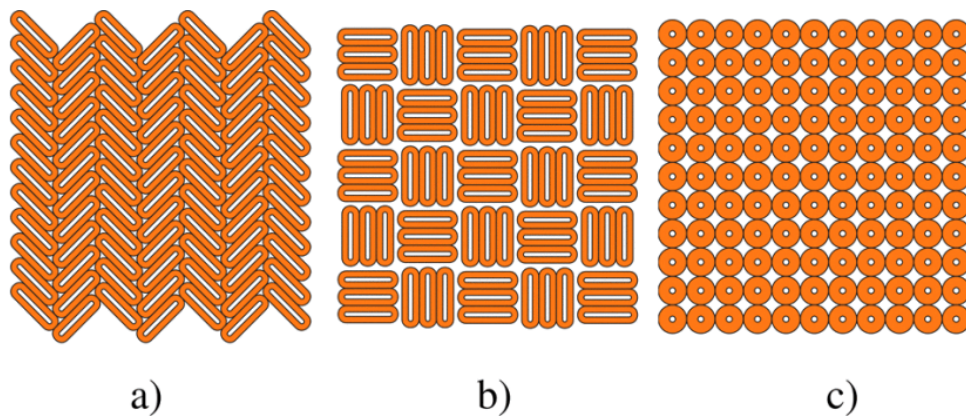


Fig. 9. A) Herringbone pattern; b) electrodynamic planar drive; c) 2D array of round coils [15]

To summarize, there are some clear differences between the 3 discussed stator topologies (see Table 1). While the stator based on several MMLM is the most straightforward with regards to its system modelling and structure, it is not meant to be modular nor extendable, thus having a limited stroke. Then, stator based on stator-long conductors has the advantages of unlimited stroke and low mechanical complexity, but it is not power efficient and more complex to control than the first topology. Lastly, stator based on 2-dimensional coil array is very modular, easily scalable and power efficient, but in standard configuration it requires a lot of components and complex system model.

Table 1. Summary of 3 most common moving magnet actuator’s stator topologies

Stator topology	Advantages	Drawbacks
MDOF stator based on several MMLM	Low number of parts. Low complexity system model.	Non-modular. Non-extendable. Limited stroke. Not very power efficient.
Stator based on stator-long 1D conductor assemblies	Low number of parts. Unlimited stroke. Topology tried and tested on a PCB.	Non power efficient. Difficult to control precisely.
Stator based on 2D coil array	Modular and scalable. Power efficient. Good controllability.	A lot of system components. Complex system model.

In the end, there are a number of ways to approach an electromagnetic system modeling of PCB-based coil arrays for a moving magnet actuator’s stator. The method to be employed is influenced by the selection of the stator’s topology, together with the chosen balance between accuracy, performance, system complexity and cost. In some instances, it is enough to construct a simple analytical system model using Lorentz force law. Fully analytical models such as those based on Lorentz force law are computationally fast and can be used for real-time system control. It is also possible to analyze such systems using finite-element method, which provides a quick way to analyze the behavior of the system. However, for building accurate and efficient systems with high level of stability, it is necessary to consider coil edge-effects, eddy current damping, thermal behavior and mechanical deformations, to name a few. Most common strategy among researchers developing similar systems is the following [7, 10, 13, 15, 22]:

- Building an analytic or semi-analytic system model.
- Building a numerical model using FEM software and comparing the obtained results.
- Building analytic system dynamics model.
- Building a system controller.
- Building a physical prototype, performing experiments and comparing the experimental results with results obtained through analytic and numerical modelling.

In this work however, only a numerical model will be considered, as complete dynamics of the system to be built is not going to be analyzed at this stage. Consequently, system controller is going to be very primitive, built to demonstrate a proof-of-concept PCB-based electromagnetic planar drive. Finally, the prototype of the stator will be built, allowing to validate the results obtained from the numerical model.

3. Practical Considerations for PCB-Based Stator

As the thesis is focused not only on the development but also on the analysis of physically constructed prototype of a PCB-based moving magnet actuator, it is crucial to consider some physical limitations which might be imposed by processes, materials, or costs of manufacturing a PCB. In fact, some of the key design challenges when developing a PCB-based electromagnetic drive system are based on the limitations imposed by the PCB manufacturing process. Considering this, standard printed circuit board manufacturing process and its limitations are overviewed here.

3.1. PCB Manufacturing

To start with, some important manufacturing limitations relating to printed circuit boards should be considered. A standard printed circuit board (Fig. 10) is composed of a rigid, non-conductive substrate core made of a glass reinforced epoxy (FR4), conductive copper tracks, non-conductive prepreg in between cores of a multi-layer PCB, and a thin insulating layer of soldermask, which serves as the top-most and bottom-most layer insulator from the environment [23]. It is also possible to have the PCB core made of metal (i.e., aluminum), ceramics (i.e., aluminum oxide or nitride), depending on the requirements dictated by the application. Then, planes of copper foil to be etched and made into conductive tracks can be distributed across one, two, or multiple layers, characterizing the PCB as a single, double, or multi-layer one.

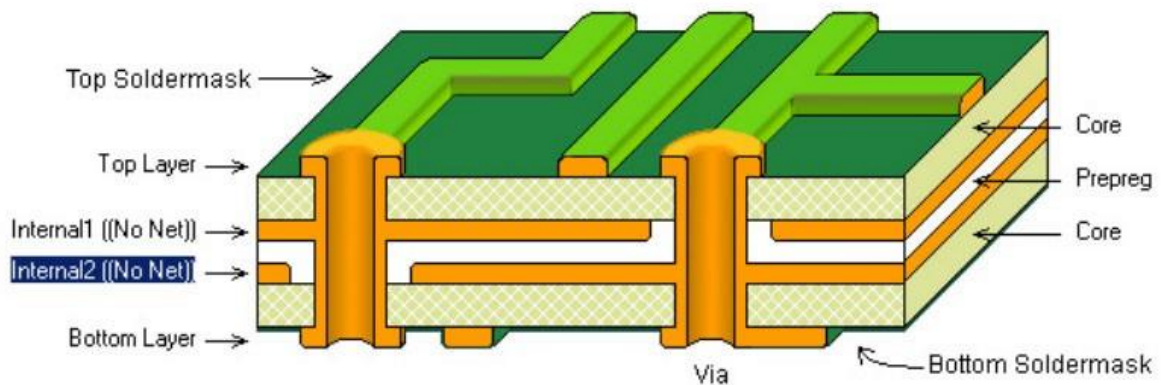


Fig. 10. Standard composition of a multi-layer PCB [24]

When it comes to manufacturing capabilities of present-day PCB makers, they can manufacture boards with extremely high precision and ever smaller features. Relevant manufacturing capabilities to this work are minimum via size, board thickness and layer number, maximum and minimum copper layer thickness, minimum track width and spacing in between them, and PCB material thermal properties. Table 2 presented below was built to compare and contrast what manufacturing capabilities 3 of the most popular PCB makers have. Additionally, each manufacturer's website was employed to obtain the pricing for one very basic PCB option, and one custom PCB option that might be relevant to this work.

Table 2. Comparison of three widely used PCB manufacturers, performed in November of 2021

	JLCPCB [25]	PCBWAY [26]	Eurocircuits [27]
Number of layers	1-6	2-40	1-16
Board thickness	0.4/0.6/0.8/1.0/ 1.2/1.6/2.0mm	0.21-6.0mm	0.20-3.2mm
Max. board size	400*500mm	508*889mm	425*425mm
Base material	FR4 (up to Tg155), Aluminum	FR4 (up to Tg220), Ceramic, PTFE, Polyimide, Aluminum	FR4 (up to Tg150), Aluminum.
Dimension tolerance	±0.2mm	±0.1mm	±0.1mm
Outer layer copper	1-2oz	1/3-7oz	1/3-3oz
Inner layer copper	0.5oz	1/3-7oz	1/3-3oz
Min. drill hole size	0.2mm	0.1mm	0.1mm
Blind/Buried Vias	No	Yes	Yes
Min. Via diameter	0.4mm	0.3mm	0.3mm
Via to Via clearance	0.254mm	0.15mm	0.1mm
Via to Track	0.254mm	0.15mm	0.1mm
Min trace & space	Inner: 0.127mm 1oz outer: 0.09mm 2oz outer: 0.20mm	0.050mm	0.090mm
Pricing			
4 layers, 100*100mm, FR-4, 1.6mm PCB thickness, 10 units, the rest of the options are to minimize cost	1.20 euro per PCB	4.20 euro per PCB	30.59 euro per PCB
100*100mm, FR-4, 10 units, other options are custom	21.13 euro per PCB (6 layers, 2mm PCB thickness, 0.5oz inner 2oz outer copper, Tg155)	26.60 euro per PCB (6 layers, 2mm PCB thickness, 1.5oz inner 2oz outer copper, Tg150-160)	158.38 euro per PCB (6 layers, 2mm PCB thickness, 2oz inner 2oz outer copper, Tg145-150)

3.2. Electromagnetic Analysis of PCB-Based Flat Coils

The aim of this section of the project is to determine the best starting point for a flat electromagnetic coil design, which can then be improved upon through FEM analysis, and eventually employed to construct a PCB-based electromagnetic drive stator. Having PCB makers' manufacturing capabilities in mind, several research and engineering projects relating to flat electromagnetic coils can now be analyzed. This aims to reveal how PCB coil design characteristics, such as copper thickness, outer diameter, inner diameter, track width and spacing, and PCB layer number, in practical terms affect the magnetic field strength and thermal performance.

As a starting point, a magnetic MEMS actuator based on parallel planar micro coil by Majlis et al. [28] was analysed. With this type of coil (Fig. 11, a), the team managed to produce a maximum of 6.8mT magnetic flux at 0.5A with 1oz copper layer, when the track width was 50 μ m, spacing 100 μ m, outer diameter 4mm, inner diameter 2.5mm. In a later paper [29], using the same coil, as well as its alternative version (Fig. 11, b), they explored what actuation force and displacement can be achieved with such coils. Using FEM analysis, as well as experiments, they demonstrated that planar spiral micro coil can produce approximately 3 times more force for the same space, width and diameter parameters. The best achieved result with experimental setup depicted in Fig. 12 showed 0.013mm displacement. It was performed at 0.2mm distance from permanent magnet to the planar coil, with 0.02mm silicone membrane resisting motion, using 1A input current, 0.1mm width, 0.1mm space spiral coil.



Fig. 11. Micro electromagnetic coils analyzed by Majlis et al. [29]: a) parallel planar circular coil; b) spiral planar circular coil

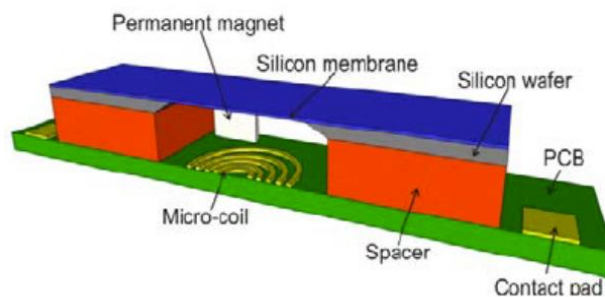


Fig. 12. Structure of MEMS actuator using PCB micro-coil developed by Majlis et al. [29]

Another work by Meydan et al. [30] looked at 4 distinct coil topologies for the use in inductive sensing, where the coils are PCB-based (Fig. 13). While it is a different use-case from this project, it can aid in better understanding magnetic field distribution and the effect of flat coil topology on it. The group of researchers analyzed the performance of circular, meander, square, and mesh flat coil topologies fitting into the perimeter of 25mm square, with 0.5mm track width, different spacing, and 0.035mm copper thickness. The results of their experiments demonstrated that coil topology strongly affects the system performance, especially its reach. To illustrate, square and circular coils showed much larger magnetic field reach when compared to the other two topologies, with the maximum result of ~10mm by the square coil, and minimum result of ~2.5mm by the meander coil.

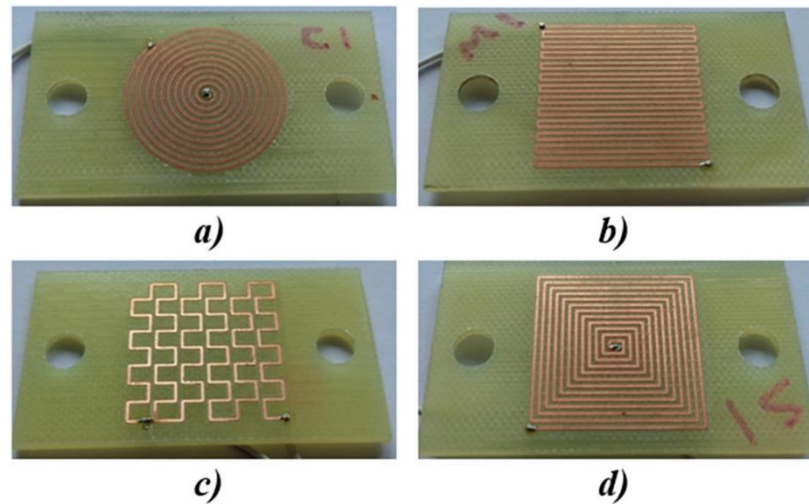


Fig. 13. Flat coils for inductive sensing by Meydan et al. [30]

Another important work on this topic explored prior to performing personal FEM analysis was the practical experiments with flat PCB coils performed by engineer Carl Bugeja on his *Youtube* channel [31]. The experiments carried out by Bugeja were with different coil configurations based on 0.1-0.3mm flexible PCBs, with 0.1mm track width and spacing, and 0.0175mm copper layer thickness. Most of the 1D actuators developed by Bugeja were 15mm to 20mm in size, with 20Ω to 40Ω resistance, drawing 0.125-0.25A of current at 5V (Fig. 14). The created coils managed to develop up to 1.96mT magnetic flux density without exceeding 90°C temperature limit (Fig. 15).



Fig. 14. Coil topologies of new PCB coil actuators by Carl Bugeja [31]

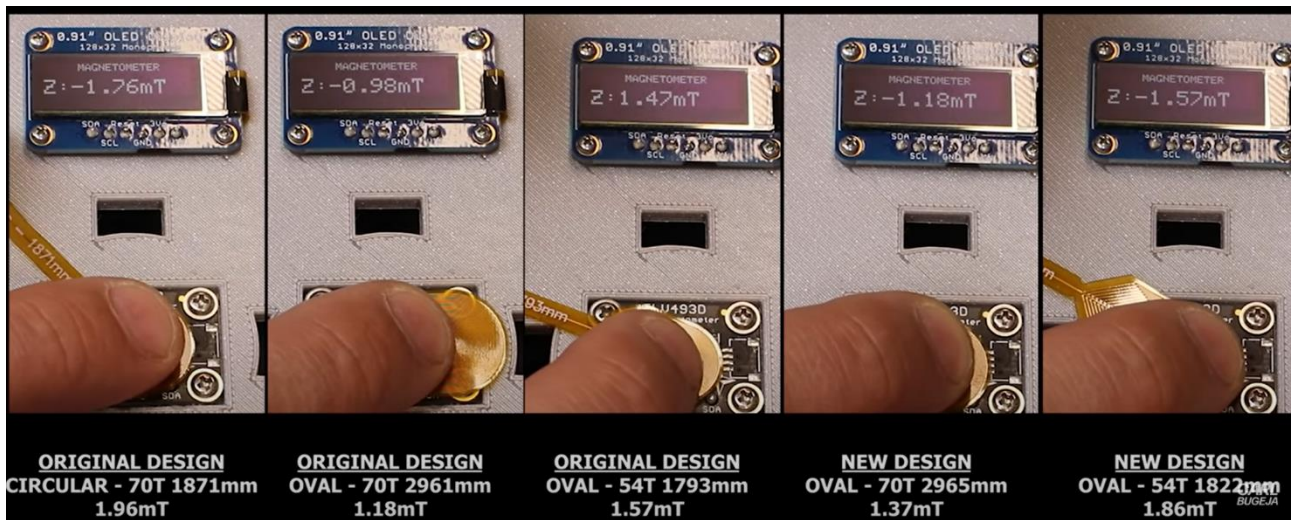


Fig. 15. Maximum magnetic flux density reached by the flat coils designed by Carl Bugeja [31]

The work presented by Carl Bugeja demonstrated that for an individual flat coil, best results are achieved by the circular coil design. Following this, some additional experiments were performed using only the circular coil. Firstly, Bugeja’s findings show that the magnetic flux density can be increased by up to 155%, if mild steel backing is applied (Fig. 16). This is beneficial when the actuated object is not a magnet, but detrimental when the interacting object is composed of permanent magnets. Next, Bugeja developed a similar flat coil on a 12-layer rigid printed circuit board, with 10Ω resistance, 0.2mm track width and spacing, which produced a magnetic flux density close to 11mT, reaching 137°C at a set voltage of 5V. Subsequently, he demonstrated that it can achieve a large actuation force in combination with a permanent magnet. For comparison, a solenoid rated at 25N was tested, reaching 20mT magnetic flux density at 5V (or 46mT at 12V), which allows to conclude that a PCB-based flat coil could potentially produce up to 13N of force, if better thermal dissipation is provided.

Core Material	Inductance	Maximum Magnetic Flux Density @ 0mm	
Flexar (No Core)	28uH	1.96mT	
Flex Ferrite Sheet (Smaller Area)	30uH	3.14mT	+60%
Flex Ferrite Sheet (Larger Area)	47uH	3.92mT	+100%
Iron (Smaller Size)	38uH	4.41mT	+125%
Iron (Larger Size)	38uH	4.12mT	+110%
Mild Steel (Smaller Size)	34uH	5.00mT	+155%
Mild Steel (Larger Size)	34uH	4.31mT	+120%
Flexar Hollow (No Core)	30uH	1.37mT	
Ferrite Core (Smaller Size)	33uH	1.86mT	+36%
Ferrite Core (Larger Size)	35uH	2.25mT	+64%

Fig. 16. Comparison of achieved magnetic flux density by different configurations of flat coils [31]

4. Development of PCB-Based Electromagnetic Drive Stator

In order to develop a PCB-based electromagnetic drive, several steps will be taken. Firstly, a single PCB-based coil will be developed through using finite element modelling method. This stage of work will help in determining the most suitable flat coil design later to be used for the electromagnetic drive. Next, testbed and control electronics will be designed and built, allowing to perform experiments and evaluate the accuracy of the theoretical model for the single coil. Lastly, control algorithm will be derived and programmed into a micro-controller, which will conclude the preparation stage and allow to test motion-related characteristics.

In the first chapter of this work, different electromagnetic planar drive topologies were overviewed. Between the 3 most common topologies – planar motion based on several linear motors, planar motion based on stator-long conductors, and planar motion based on an array of coils – the latter demonstrated the biggest potential for further investigation for the use as a PCB-based stator. It is due to the most flexibility regarding the stator layout, as well as concentrated magnetic field with high efficiency, when compared to the stator long conductors.

4.1. Modelling of a Single Flat Coil

4.1.1. FEM-Based Electromagnetic Analysis of PCB Flat Coils

Core electromagnetic parameters

Firstly, it is important to know which factors will have the greatest influence on electromagnetic and thermal performance of the PCB based stator. To begin with, the magnetic field produced by current carrying conductor can be expressed by using Ampere's law:

$$B = \frac{\mu_0 I}{2\pi r} \quad (1)$$

where μ_0 is permeability of free space (N/A^2), I is current in a wire (A), r is radial distance from the wire (m).

As can be seen by Ampere's law, the magnetic field is directly proportional to the current in the wire and inversely proportional to the distance from it. Then, another important consideration can be taken from Joule-Lenz law, which states that heat generated in a conductor will be directly proportional to square of the current and conductor's resistance:

$$P \propto I^2 R \quad (2)$$

Next, the resistance itself is inversely proportional to the area of the conductor, which means that higher copper thickness will result in lower ohmic losses:

$$R = \rho \frac{L}{A} \quad (3)$$

where L is the length of the conductor (m), A is its cross-sectional area (m^2), ρ is material's resistivity ($\Omega \cdot \text{m}$).

Considering the work done by Majlis et al. and Carl Bugeja, a starting point for further work will be 12mm external diameter, 1.6mm PCB thickness and 0.5A input current. These parameters will be

varied one by one in order to find the influence of each of them to the stator coil's electromagnetic performance. The comparison will be performed using *COMSOL Multiphysics 5.4* magnetic fields and heat transfer in solids packages. The results of the FEM modelling are summarized and presented in Table 3. A coil used as a starting point can be seen in Fig. 17.

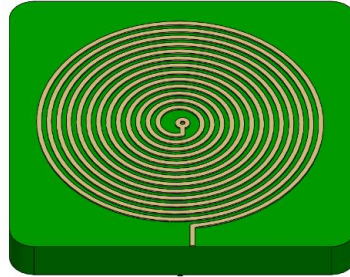


Fig. 17. A single coil to be used in FEM simulations - 12mm outer coil diameter, 0.07mm copper layer thickness, and 0.2 mm track width and spacing on a 1.6mm thickness PCB

Table 3. Summary of PCB-coil modelling results using FEM, at 0.5A input current

Changing parameter	Input					Output			
	Track width & spacing (TWS)	Copper thickness (CT)	Copper layers (CL)	Outer coil diameter (OD)	Inner coil diameter (ID)	B [mT]	T [°C]	R [Ω]	H [mH]
CT	0.2	0.018	1	12	n/a	5	163	1.29	0.72
	0.2	0.035	1	12	n/a	4.5	94	0.66	0.72
	0.2	0.07	1	12	n/a	3.8	57	0.33	0.71
TWS	0.1	0.07	1	12	n/a	7.7	165	1.33	2.83
	0.2	0.07	1	12	n/a	3.8	57	0.33	0.71
	0.4/0.2	0.07	1	12	n/a	2.5	32	0.11	0.3
	0.4	0.07	1	12	n/a	2	21	0.08	0.18
CL	0.2	0.07	1	12	n/a	3.8	57	0.33	0.71
	0.2	0.07	2	12	n/a	4.6	91	0.65	1.88
	0.2	0.07	4	12	n/a	8.15	222	1.93	7.73
ID & CL	0.2	0.07	2	12	4	4	82	0.59	1.66
	0.2	0.07	4	12	4	5.8	139	1.17	6.84
OD & CL	0.1	0.035	2	6	n/a	8.7	211	1.3	1.02
	0.1	0.035	2	4	n/a	7.3	84	0.6	0.3
	0.1	0.035	1	4	n/a	7	58	0.3	0.1

Copper thickness

Firstly, the copper thickness effect on the magnetic field strength and coil temperature was analyzed. Common copper layer thicknesses are 0.5oz, 1oz and 2oz, which translates into 17.5µm, 35µm and 70µm layer of copper respectively. All three options were simulated and the results are presented in CT section of the Table 3. As expected, with increasing layer thickness, coil resistance and maximum reached temperature decrease. However, the magnetic flux density is also decreasing, even though it is supposed to stay close to constant with a constant current. Further exploration of this discrepancy might be needed.

Track width and spacing

Next, track width and spacing have a big influence on the magnetic and thermal coil performance. Since the coil diameter is kept constant, with bigger track width and spacing, there is less track length and less windings, which directly affects coil resistance, inductance, magnetic flux density and thermal performance. A summary of results is presented in TWS section of the Table 3, which demonstrates that all parameters are strongly reduced with increasing track width and spacing.

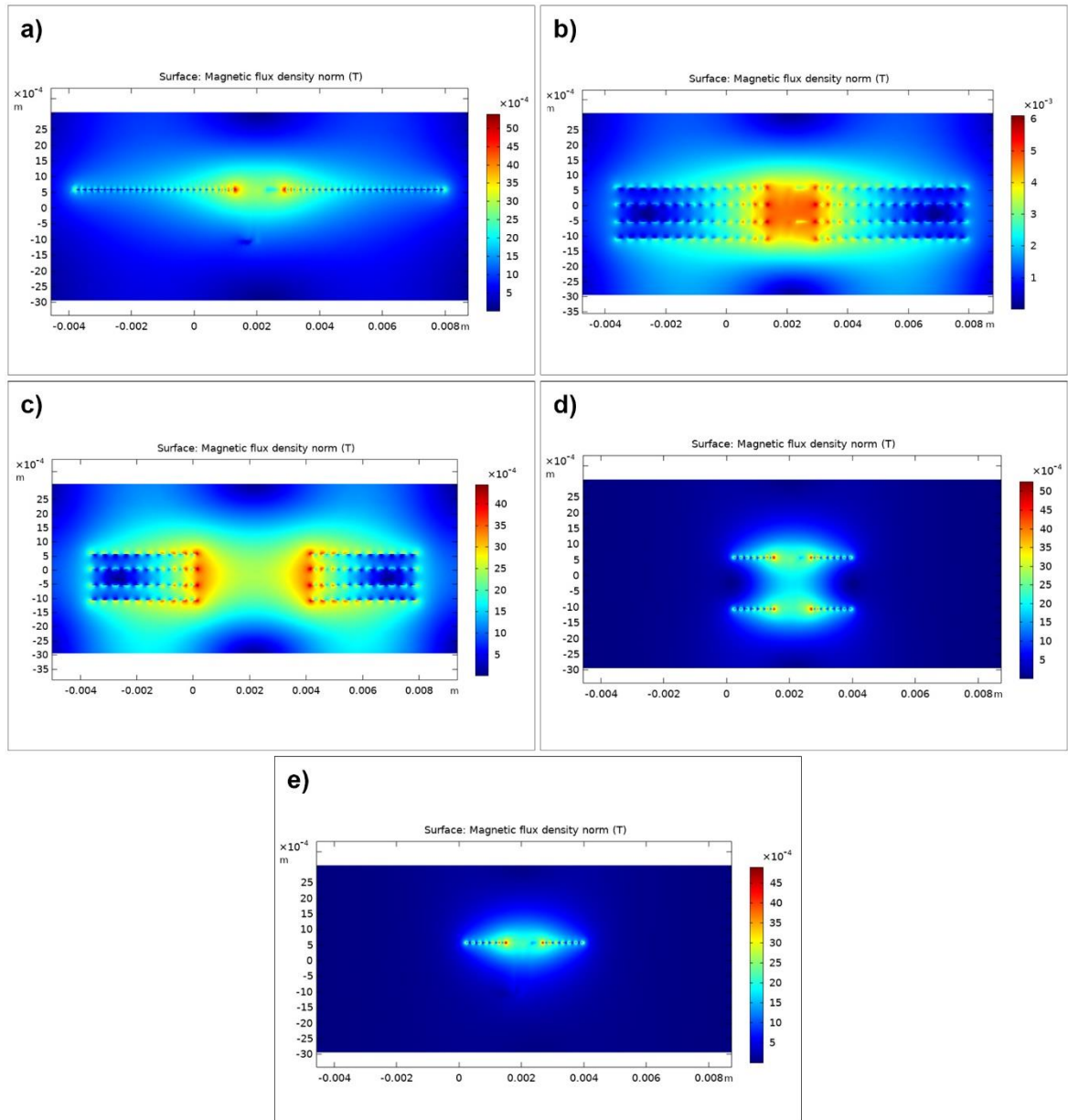


Fig. 18. FEM simulation results for different coil configurations with the highest magnetic flux density, showing its distribution around each coil: 12mm OD, 7.7mT & 165°C (top left), 12mm OD, 8.15mT & 222°C (top right), 12mm OD 5.8mT & 139°C (middle left), 4mm OD, 8.7mT & 211°C (middle right) and 4mm OD, 7mT & 58°C (bottom)

Layer number

The next parameter which has an effect on magnetic and thermal properties of the coil is the number of coil layers. Additional layers contribute to strengthen the magnetic field of the initial layer, while

at the same time increasing overall coil resistance, inductance and maximum temperature. A summary of simulation results with 1, 2 and 4 identical coil layers is presented in CL section of the Table 3.

Other

From the previous results it could be observed that most of the magnetic field is concentrated in a small portion within the center of the coil (Fig. 18). For this reason, two more coil variations were analyzed, attempting to make the field above the coil more uniform. Firstly, inner diameter was added, reducing magnetic flux density, resistance, inductance and maximum temperature when compared to the same coil design without the inner diameter (see ID & CL section of the Table 3). Next, outer diameter was reduced, which resulted in more balanced magnetic field distribution with high flux density and good thermal performance (Fig. 19) (see OD & CL section of the Table 3). This demonstrated that wider coil at its edges does not make a significant enough contribution to overall magnetic flux density, especially with small layer number.

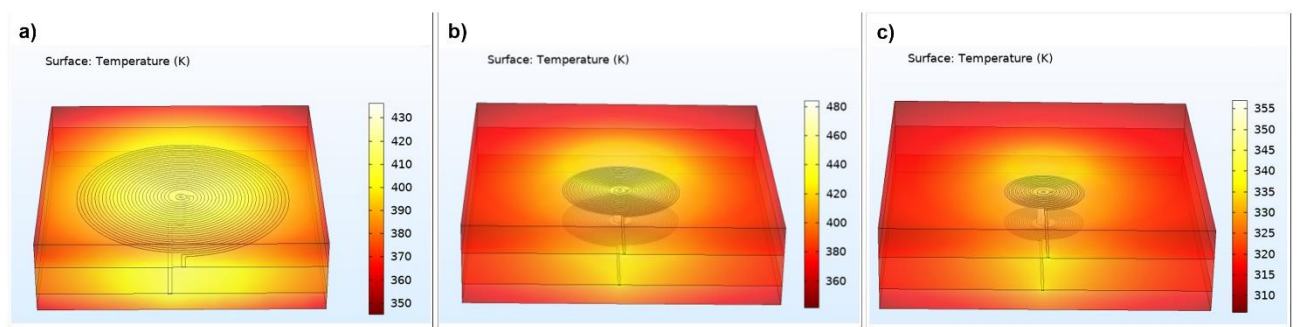


Fig. 19. Simulated thermal performance of a PCB-based flat coil with varying parameters: a) maximum temperature of 165°C with 12mm OD on 1 layer (0.07mm CT); b) 211°C with 6mm OD on 2 layers (0.035mm CT); c) 84°C with 4mm OD on 2 layers (0.035mm CT).

Finite element method analysis results demonstrated that a small PCB-based coil can achieve up to 7.3mT magnetic flux density without exceeding standard PCB temperature limit (T_{g155}) with 0.5A current. However, this could still be improved upon by adding a heatsink and increasing the supplied current. Based on an off-the-shelf solenoid described in subchapter 3.2, thermally optimized PCB-based coil with 4mm outer diameter could be expected to achieve approximately 10N of pulling/pushing force at its surface. Furthermore, the obtained results are in close agreement with what Majlis et al. [7] discovered in their research, as well with Carl Bugeja's experimental results.

4.2. PCB-Based Stator Testbed Development

Up to this point, the groundwork allowing to begin designing a physical PCB-based testbed was laid out. To quickly sum up, previously discussed 2D array of coils stator topology was chosen; similar types of work and PCB manufacturing limitations were discussed, allowing to perform FEM simulations to determine the best single flat PCB-based coil design. Now, a physical testbed for testing the obtained results in practice will be designed and built. In addition to testing the results of FEM simulations, 3 types of stators will be built to test if the hypothesized ideas at the beginning of this work are valid – if a single PCB-based flat coil can be arbitrarily patterned to achieve different types of motion, such as linear, rotary and planar.

Firstly, an isolated flat coil will be placed on the PCB for checking of the validity of results obtained using FEM. Two different versions of isolated coil will be used (Fig. 20, top): single layer, 4mm outer diameter, 0.1mm track width and spacing, 0.035mm layer thickness; double layer (two consecutive layers on a 4-layer PCB), with same OD and TWS, but the internal PCB layer, due to manufacturing limitations, will have to be 0.0175mm thick. These two coils will be connected directly to a precision DC laboratory power supply, thus allowing to set the necessary voltage to reach the desired current flow.

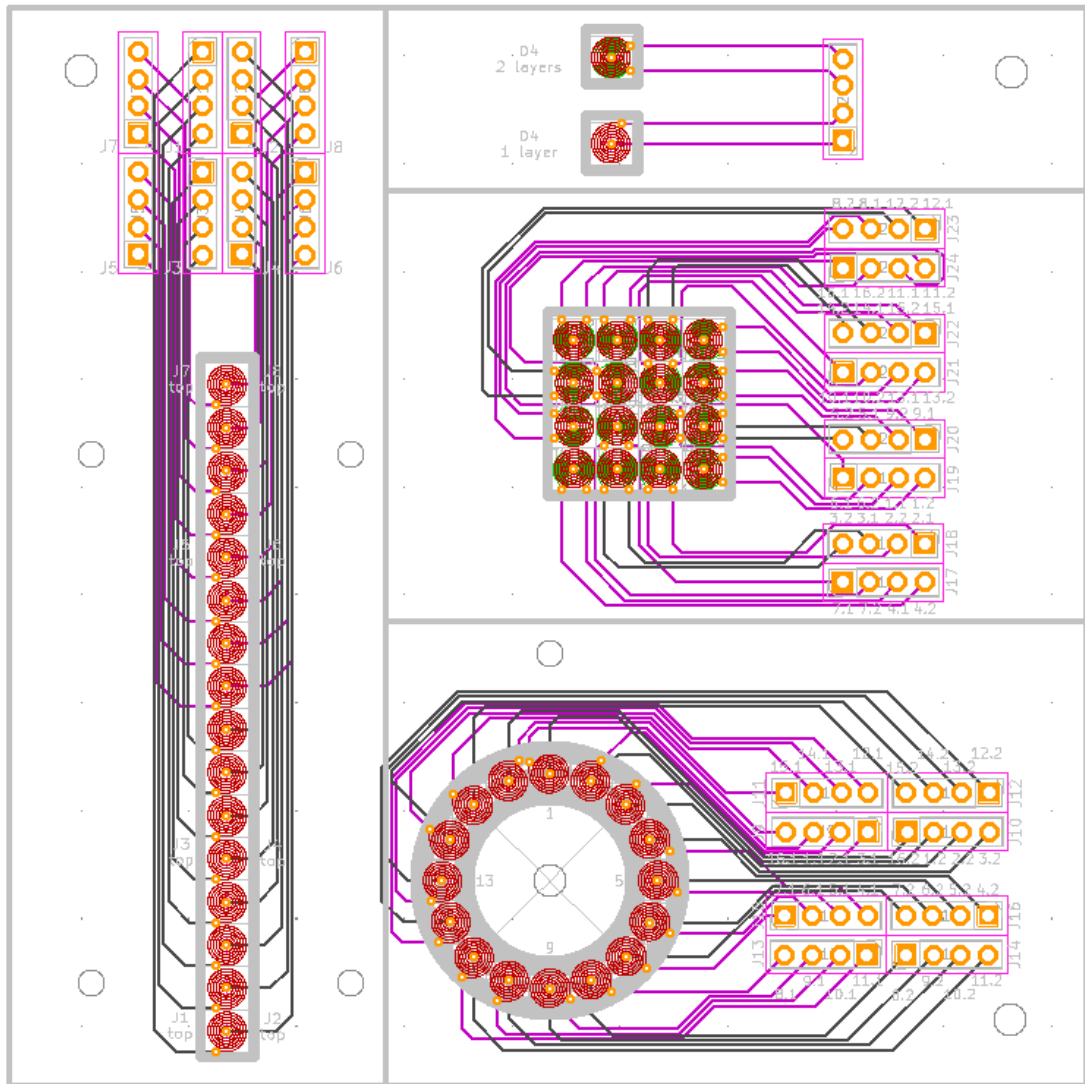


Fig. 20. PCB view of stators tested: two separate flat coils (top), linear drive stator configuration (left), rotary drive stator configuration (bottom), and planar drive stator configuration (middle)

Next, a linear and rotary drive set-up will be developed (Fig. 20, left). For the linear drive, a single row of 16 coils will be implemented, resulting in a 64mm long and 4mm wide strip of flat coils. For the rotary drive, 16 coils will be patterned around 30mm diameter circle. Such configurations, as well as all the subsequent ones, will require control electronics implemented. For initial tests, a single direction of current flow will be sufficient, allowing to either have attractive or repulsive coils, but not both. To achieve this, a microcontroller and 16 MOSFETs will be required. At this point, system will be open loop, which means no more components will be necessary.

Finally, a configuration for a planar drive will be implemented (Fig. 20, middle). It is the final and the most important configuration, which serves as a proof of concept for electromagnetic planar drive with untethered mover. It will be composed of 4-by-4 matrix of 2-layer coils, with its control electronics based on the same setup as for the linear and rotary drives. This will firstly allow the testing of 2D untethered movement, with the potential to extend the tests up to 6 degrees of freedom.

To achieve all three motion configurations described previously, in addition to the testboard PCB, only two other types of electronic components will be necessary: a microcontroller and 16 identical MOSFETs. A microcontroller to be employed can be any generic microcontroller which is capable of supplying logic level voltage on at least 16 outputs. For this reason, a readily available *STM32F103C8T6* development board with 37 general purpose input-output pins was selected [32]. It is 3.3-5V tolerant, and *Arduino IDE* compatible, which makes it extremely simple and quick to deploy for such a scenario. In addition to the microcontroller, 16 logic-level gate drive enhancement type MOSFETs, with at least 1A continuous drain current capability will be needed. For this, *IRLML2502PbF* power MOSFET was selected [33]. It can handle up to 4.2A continuous drain current, with a maximum of 1.2V gate threshold, and has only 0.045Ω on-resistance. A schematic view applicable to linear, rotary and planar configurations is depicted in Fig. 21.

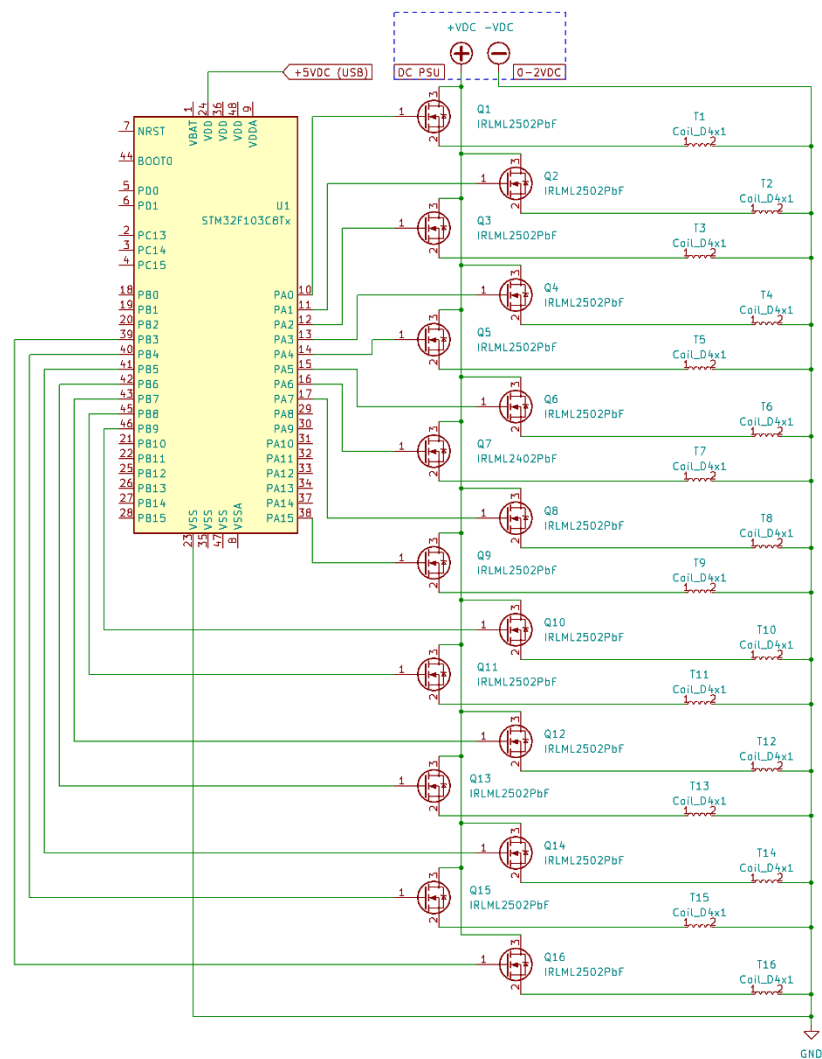


Fig. 21. Schematic view of electronics setup applicable to linear, rotary, and planar drives configurations

In addition to the printed circuit board testboard, two types of movers with magnets were developed. For the isolated coil testing, the following neodymium magnets will be used (Fig. 22, a): 4 by 4 by 2mm, N42; 5 by 5 by 1.2mm, N50; D5 x 2mm, N52; 3 by 3 by 3mm, N42. For the linear motion, the magnet which performed best on isolated coil tests and is of sufficient size will be employed. Then, same magnets but with different magnet and housing combinations will be used for the remaining two tests (Fig. 22, b): 2 magnets on opposing circle sides for rotary motion, and 4 magnets on corners of a mover, separated by 2 coil diameters center-to-center from each other for planar motion.

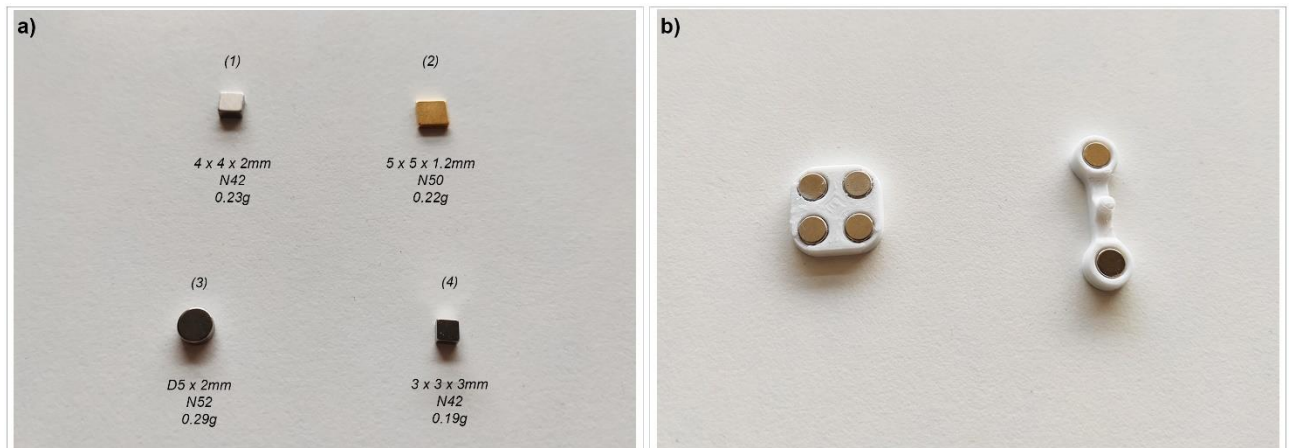


Fig. 22. a) 4 magnets for individual flat coil tests; b) two movers with selected type of magnet (nr. 3), one for planar motion testing (left) and one for rotary motion testing (right)

5. Experiments With PCB-Based Stators for an Electromagnetic Drive

Having the PCB-based stator testbed developed (Fig. 23), experiments can now be performed. This testbed will be employed, in conjunction with some control electronics, to test 4 different usage scenarios for a PCB-based coil. The first use case will be as an isolated coil, which will test the payload capacity of a single-layer and two-layer coils, also allowing to evaluate the validity of the FEM simulations. Next, linear and rotary motion will be tested, attempting to establish smooth controllable motion and evaluate positioning resolution, as well as mover's linear speed and revolutions per minute. Lastly, 2-dimensional movement will be tested, evaluating if this PCB-based topology could work as a planar electromagnetic drive.

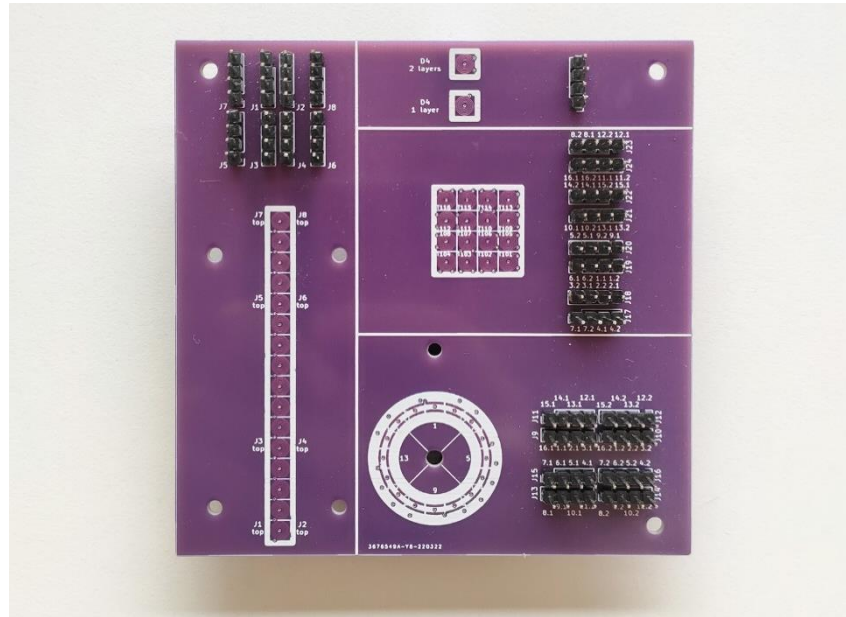


Fig. 23. A testbed of stators developed for PCB-based electromagnetic drive experiments

5.1. Experiments With Individual Coils

Firstly, static parameters, such as electrical resistance, magnetic flux density, maximum temperature and payload capacity were evaluated. It was done through working on the top-right zone with two individual coils on the PCB testbed, in combination with neodymium magnets and some extra masses. The results of the tests are presented in Table 4 below and within two graphs depicted in Fig. 24. Additionally, testing procedures, tools and results are described in the remainder of this subchapter.

Table 4. Experimentally obtained resistance, temperature and magnetic flux measured for individual coils

	R [Ω]	T [°C] (at 0.5A)	B [mT] (at 0.5A)	I_{max} [A] (at 145°C)
Single-layer coil	0.4	47	0.6	1.10
Single-layer coil with heatsink	0.4	35	0.6	1.25
Two-layer coil	1.0	84	0.9	0.60
Two-layer coil with heatsink	1.0	66	0.9	0.85

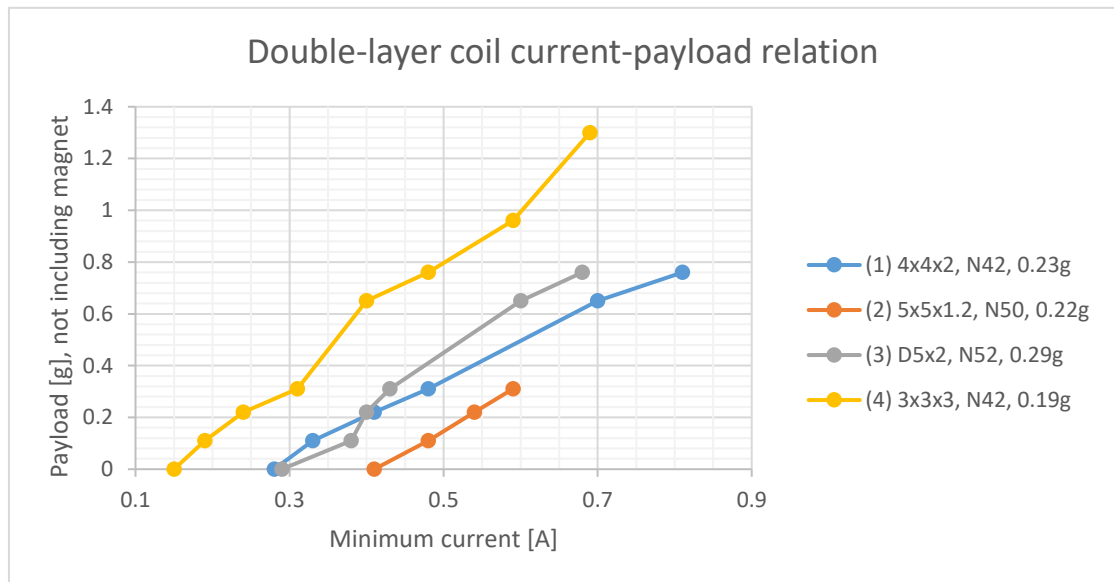
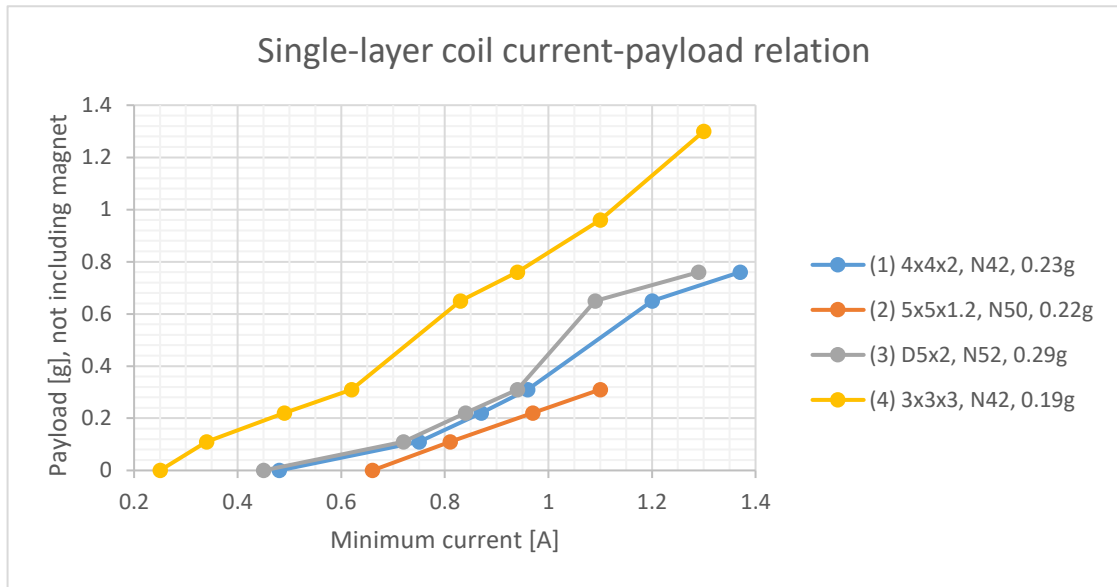


Fig. 24. Current to payload relation for single-layer (top) and double-layer (bottom) coils with 4 different magnets

Resistances of the coils were measured using *Proster VC99* multimeter (Fig. 25, b) [34], with resolution of 0.1Ω and accuracy of $\pm(0.8\%+3)$ [34]. 5 identical PCB boards were measured, with the resistances ranging from 0.3Ω to 0.5Ω for the single layer-coil and from 0.8Ω to 1.2Ω for the two-layer coil. Then, temperature was observed for both coils, allowing it to settle for 1 minute while passing a $0.5A$ current through them. *Seek Shot* thermal imaging camera (Fig. 25, c) [35], with $0.07^\circ C$ thermal sensitivity was used to capture the temperatures and their distribution, while *LongWei PS3010DF* precision laboratory power supply (Fig. 25, d) [36] with $\leq 0.1\% + 10mA$ accuracy was employed to supply the needed current. Maximum temperature reached for single-layer coil was $47^\circ C$, while double-layer coil reached $84^\circ C$ (Fig. 26). Additionally, a small aluminum heatsink was attached to the backside of the PCB directly under the coils, which reduced the maximum temperature down to $35^\circ C$ for single-layer and down to $66^\circ C$ for double-layer coil.

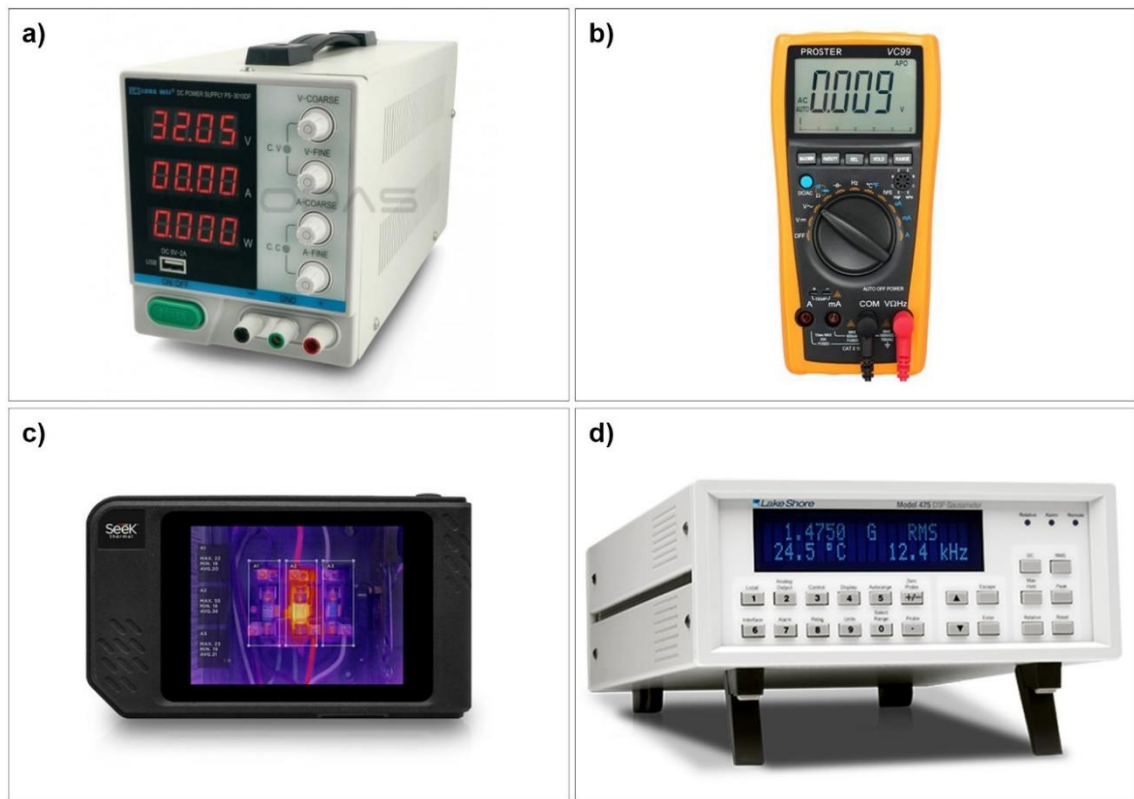


Fig. 25. Main equipment used for the experiments: a) *LongWei PS3010DF* precision laboratory power supply [37]; b) *Proster VC99* multimeter [34]; c) *Seek Shot* thermal imaging camera [35]; d) *Lakeshore Model 475 DSP* gaussmeter [36]

Furthermore, the current limit for each coil when the temperature reaches maximum allowable PCB material temperature was obtained (for FR-4 TG155 PCB board it is 155 degrees Celsius, but to be on the safe side, 145°C was set as the limit). The current from the power supply was incrementally increased in steps of 0.1A and the temperature was allowed to settle each time for approximately 1 minute. This way, it was observed that a single-layer coil can handle up to 1.1A of current with no

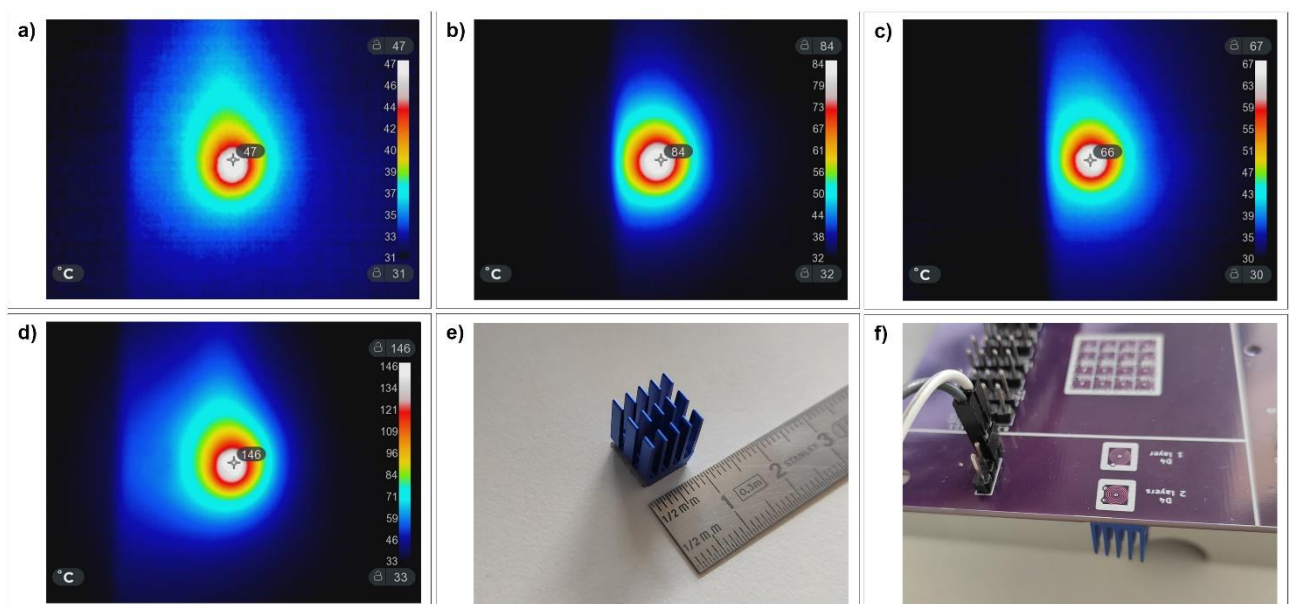


Fig. 26. Individual coil thermal tests: a) 1-layer coil at 0.5A; b) 2-layer coil at 0.5A; c) 2-layer coil at 0.5A with a heatsink; d) 1-layer coil at 1.1A; e) heatsink; f) the two individual coils with heatsink on the backside

additional heatsink, while double layer coil with the same setup can only handle up to 0.6A. With an added heatsink, the same double-layer coil could withstand extra 0.25A before reaching 145°C.

For magnetic flux density measurements, *Lakeshore Model 475 DSP* gaussmeter, with 0.35mT to 35T measuring range was utilized [36] (Fig. 25). In these measurements, direction and placement of the measuring probe (*HMMT-6J04-VR*, Fig. 27) was crucial, as the magnetic flux density is highly concentrated in small area, with magnetic field strength decreasing by distance cubed when going further from the source (same behavior as magnetic dipole). Furthermore, it is important to mention that the hall effect sensor located at the tip of the probe is from 0.29mm to 0.99mm deep from the touching surface, with an additional 0.1mm to 0.15mm added separation by the solder mask on the copper tracks. The obtained values ranged substantially between 0.2mT and 0.6mT for the single layer coil (depending on how the measuring probe was positioned), and between 0.4mT and 0.9mT for the double layer coil. In both cases, constant 0.5A of current was passed through the coils.

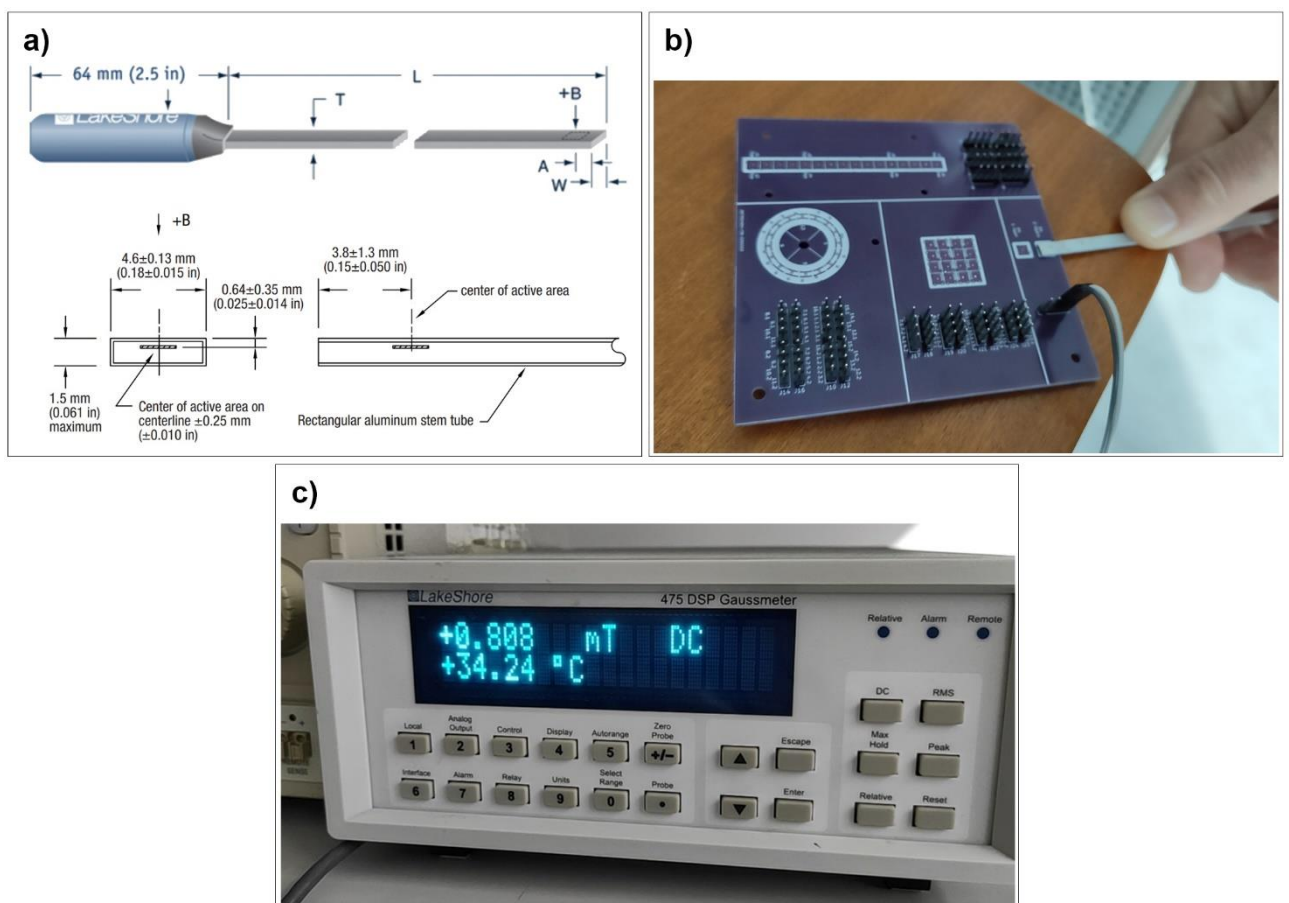


Fig. 27. Magnetic flux density test setup: a) hall effect probe with exact sensor location [36]; b) testbed with probe taking a measurement; c) Gaussmeter showing nearly maximum measurement of 2-layer coil at 0.5A

Lastly, the two graphs in Fig. 24 show how single coil payload capabilities depend on the applied current. Firstly, it was already determined that maximum current for single-layer coil with a heatsink should not exceed 1.3A, and 0.8A for the double-layer coil. However, this current should be applied for very short periods, only to allow a single test at a time, as the magnets are in direct contact with the heat source, and they have much lower demagnetization temperature than the maximum PCB temperature (65-90°C). Then, small masses weighing 0.11g, 0.31g, and 0.65g were taken to evaluate how much weight approximately each magnet can support (Fig. 28).

The experiment demonstrated that both single-layer and double-layer coils have similar maximum payload capacity of approximately 1.5g. While the current needed to achieve the same maximum value was nearly twice lower for double-layer coil (0.69A) than for a single-layer coil (1.30A), due to the difference in coil resistance, voltage needed for double-layer coil was higher, making the power consumption and stator heating nearly identical. Through the experiments, it was determined that an N42 cube magnet of 3mm per side can support the maximum payload. However, it is too small compared to coil center-to-center distance, which led to choosing 5mm diameter, 2mm height N52 magnet for all motion tests.

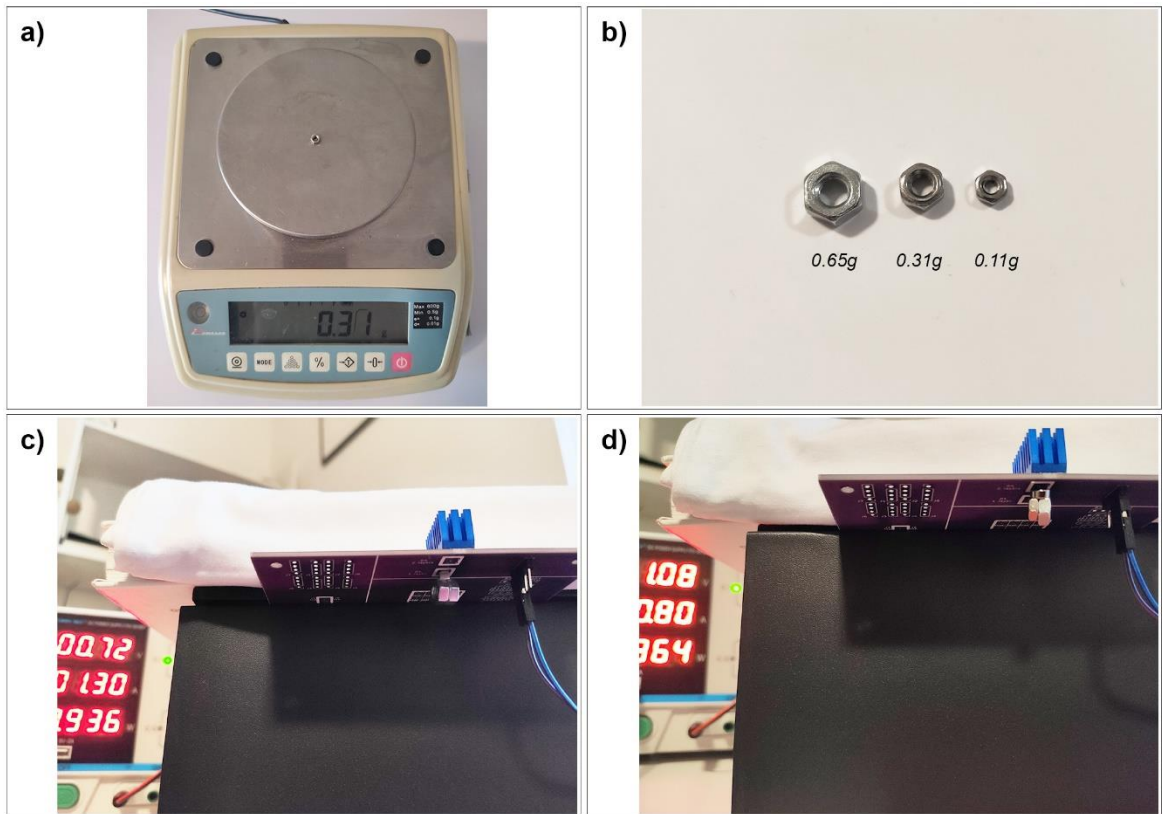


Fig. 28. Setup for payload tests: a) precision electronic scale; b) nuts used as masses; c) payload test for 1-layer coil supporting 1.5g; d) payload test for 2-layer coil supporting 1.25g

5.2. Experiments With Generating Linear and Rotary Motion

Next stage of experiments was to develop a basic 1-dimensional motion, including linear and rotary. For that, the developed PCB testbed was connected to the control electronics described in the previous chapter. Fully connected testbed prepared for the linear motion tests can be observed in Fig. 29. For rotary tests, the breadboard jumper wires connected to the linear motion part on the PCB had to be reconnected to the rotary zone of the testbed, and only the code within the microcontroller had to be changed.

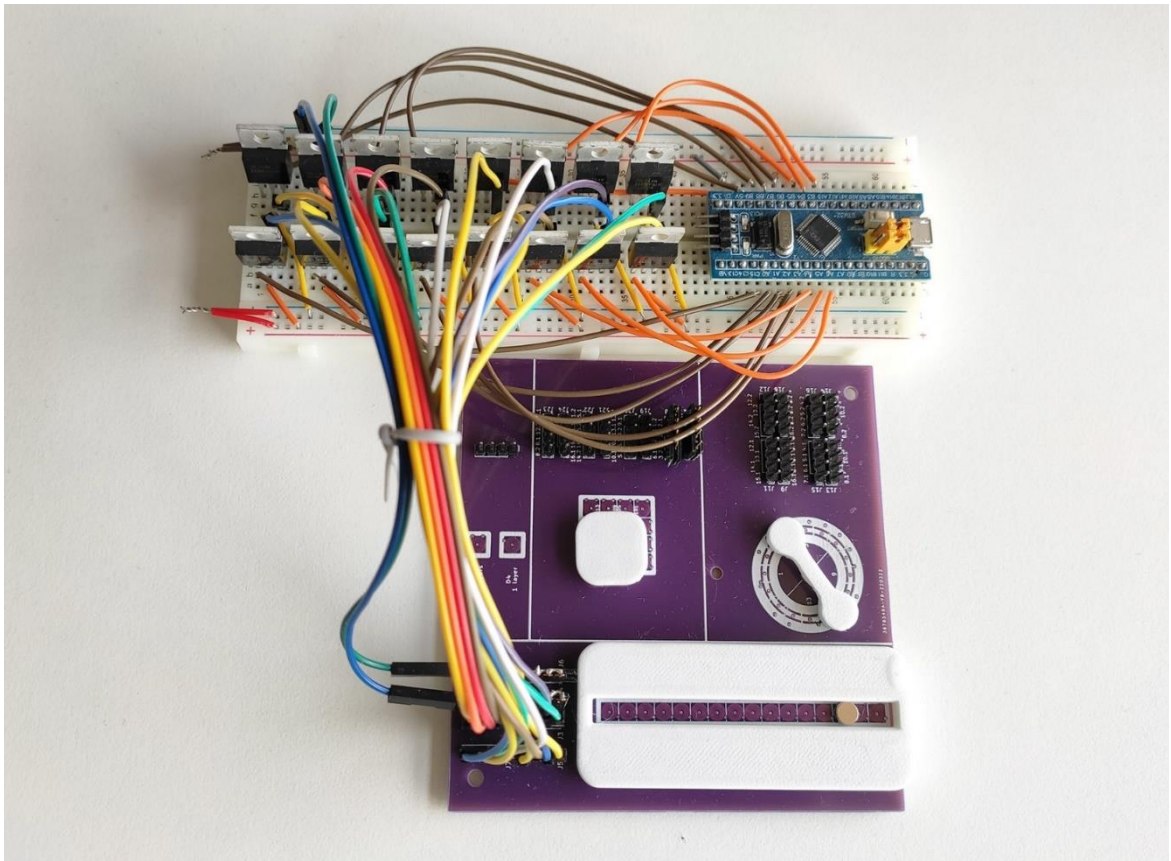


Fig. 29. PCB testbed of stators prepared for the linear motion tests

Now, in order to test if the coils can produce linear and rotary motion, code for it had to be written. As the *STM32F103C8T6* development board was chosen, C++ adapted for *Arduino IDE* was employed to program the microcontroller. For all three – linear, rotary and planar configurations, the same starting code can be used, as all 3 configurations require to set-up 16 outputs to control transistor gates. This reusable code is meant to run once, as the microcontroller is powered-on. The code is demonstrated in Fig. 30.

```

const int arraySize = 16;
int coils[arraySize] = {PA0, PA1, PA2, PA3, PA4, PA5, PA6, PA7, PA15, PB3, PB4, PB5, PB6, PB7, PB8, PB9};

void setup() {

  for (int i = 0; i < arraySize; i++) {
    pinMode(coils[i], OUTPUT);
    digitalWrite(coils[i], LOW);
  }
}

```

Fig. 30. Starting code for all three configurations tests – linear, rotary, and planar

Next, while it is very straightforward to produce basic motion in steps from coil to coil, it is rather complex to generate a code which would produce smooth and easily controllable motion. Generally, for this purpose, motor drivers are implemented, and it would not be an exception in this case. However, the amount of work needed to implement a motor driver is outside of the scope of this project. Consequently, only basic code will be implemented in order to demonstrate a proof-of-concept linear and rotary motion (Fig. 31).

One of the aims of the thesis was to achieve at least 100mm/s linear motion with a PCB-based electromagnetic drive. As the linear drive has a maximum stroke of 60mm, this requires moving the full length of it in 600ms or less. For this, starting at larger delays and working down, through trial and error it was obtained that with the delays in milliseconds depicted in Fig. 31 (a), the mover (N52 single magnet, 5mm in diameter, 2mm in height) completes full 60mm with a theoretical speed equal to approximately 100mm/s. For factual speed approximation, a video camera with millisecond timestamp was employed. It was evaluated that theoretical speed is in very close proximity to the factual speed of 101mm/s (Fig. 32).

<p>a)</p> <pre> void loop() { // 60mm forward for (int i = 0; i < 15; i++) { digitalWrite(coils[i], HIGH); delay (14); digitalWrite(coils[i+1], HIGH); delay (14); digitalWrite(coils[i], LOW); delay (7); digitalWrite(coils[i+1], LOW); delay (7); } delay (2000); // 60mm backward for (int i = 15; i > 0; i--) { digitalWrite(coils[i], HIGH); delay (14); digitalWrite(coils[i-1], HIGH); delay (14); digitalWrite(coils[i], LOW); delay (7); digitalWrite(coils[i-1], LOW); delay (7); } delay (4000); } </pre>	<p>b)</p> <pre> void loop() { // rotates one full circle clockwise for (int i = 0; i < 16; i++) { if (i<8) { digitalWrite(coils[i], HIGH); digitalWrite(coils[i+8], HIGH); delay (30); digitalWrite(coils[i], LOW); digitalWrite(coils[i+8], LOW); delay (5); } else if (i<15) { digitalWrite(coils[i], HIGH); digitalWrite(coils[i-8], HIGH); delay (30); digitalWrite(coils[i], LOW); digitalWrite(coils[i-8], LOW); delay (5); } else if (i==15) { digitalWrite(coils[0], HIGH); digitalWrite(coils[8], HIGH); delay (30); digitalWrite(coils[0], LOW); digitalWrite(coils[8], LOW); } } delay (2000); } </pre>
---	---

Fig. 31. Code for: a) basic linear motion of 60mm forward and backward; b) around a 30mm diameter circle



Fig. 32. Screen captures of a video demonstrating 100mm/s linear motion, starting at image a)

While the desired speed was achieved, it is not going to be possible through this work to achieve the desired stepping resolution. It was mentioned previously that smooth, high-resolution motion would be required to develop a custom driver, which is outside the scope of this work. However, as the principle of motion with this custom electromagnetic drive is similar to that of a conventional stepper

motor, it could be expected that some level of microstepping could be achieved. With readily available and inexpensive stepper drivers, such as *Trinamic TMC2209* [38], it is possible to achieve up to 1/256 stepping resolution, which in this case, with 4mm original step (coil center to coil center), would translate to 0.015625mm step resolution. However, this comes at the cost of lost payload capacity, which in regular rotary bipolar stepper motors would decrease to 0.61% of original at 1/256 stepping resolution [39].

When it comes to rotary motion, code was implemented to achieve 1 revolution per 0.5s, or 120rpm (Fig. 31, b). For factual rotational speed approximation, a video camera with millisecond timestamp was employed. It was evaluated that theoretically set speed is in very close proximity to the factual speed of 125rpm (Fig. 33). Then, similarly to linear motion, microstepping driver would be needed to achieve higher resolution motion. As it stands now, with 16 coils, one full step consists of 22.5 degrees. This could theoretically be lowered down with 1/256 step resolution, which would result in 0.09 degrees step.



Fig. 33. Screen captures of a video demonstrating 120rpm rotary motion, starting at image a)

5.3. Experiments With Generating 2D Planar Motion

Finally, basic planar motion was tested. It was done on a PCB testbed stator with 4-by-4 grid of two-layer flat coils, with the same electronics setup that was used for linear and rotary motion. Code was implemented (Fig. 35) to demonstrate motion around the perimeter of the grid (Fig. 34) with a 14mm-by-14mm mover with 4 magnets (N52, 5mm in diameter, 2mm in height) on its corners. It was demonstrated that at least 3 degrees of freedom motion is possible with such a setup – along x and y axes, as well as rotation around z axis. However, as was the case with linear and rotary motion, a custom driver would be needed to achieve smooth, higher resolution motion.

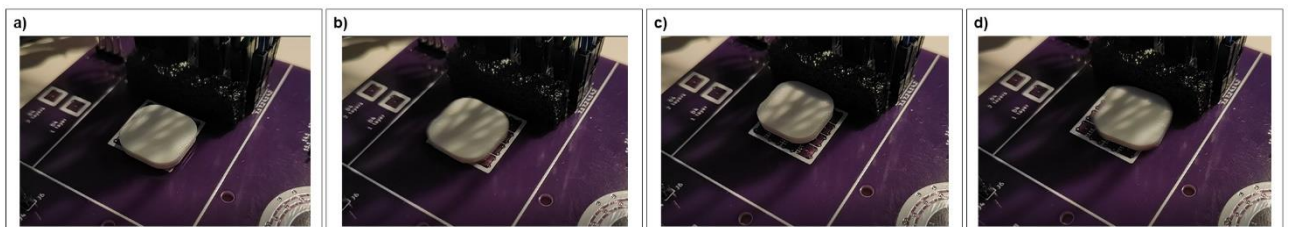


Fig. 34. Screen captures of a video demonstrating planar motion around the perimeter of 4-by-4 coil grid

```

void loop() {
  digitalWrite(coils[1], HIGH); digitalWrite(coils[3], HIGH); digitalWrite(coils[9], HIGH); digitalWrite(coils[11], HIGH);

  digitalWrite(coils[13], HIGH); digitalWrite(coils[15], HIGH); delay (20);
  digitalWrite(coils[9], LOW); digitalWrite(coils[11], LOW); delay (0);
  digitalWrite(coils[1], LOW); digitalWrite(coils[3], LOW); delay (100);
  digitalWrite(coils[5], HIGH); digitalWrite(coils[7], HIGH); delay (500);

  digitalWrite(coils[12], HIGH); digitalWrite(coils[4], HIGH); delay (20);
  digitalWrite(coils[13], LOW); digitalWrite(coils[5], LOW); delay (0);
  digitalWrite(coils[15], LOW); digitalWrite(coils[7], LOW); delay (100);
  digitalWrite(coils[14], HIGH); digitalWrite(coils[6], HIGH); delay (500);

  digitalWrite(coils[0], HIGH); digitalWrite(coils[2], HIGH); delay (20);
  digitalWrite(coils[4], LOW); digitalWrite(coils[6], LOW); delay (0);
  digitalWrite(coils[12], LOW); digitalWrite(coils[14], LOW); delay (100);
  digitalWrite(coils[8], HIGH); digitalWrite(coils[10], HIGH); delay (500);

  digitalWrite(coils[3], HIGH); digitalWrite(coils[11], HIGH); delay (20);
  digitalWrite(coils[2], LOW); digitalWrite(coils[10], LOW); delay (0);
  digitalWrite(coils[0], LOW); digitalWrite(coils[8], LOW); delay (100);
  digitalWrite(coils[1], HIGH); digitalWrite(coils[9], HIGH); delay (300);

  digitalWrite(coils[1], LOW); digitalWrite(coils[3], LOW); digitalWrite(coils[9], LOW); digitalWrite(coils[11], LOW);
  delay (5000);
}

```

Fig. 35. Code for looping planar motion around the perimeter of the 4-by-4 coil grid

6. Discussion

Up to this point, a PCB-based stator topology consisting of a 2D array of flat coils for a custom electromagnetic drive was analyzed both theoretically, using FEM, and experimentally, on a custom PCB testbed. The FEM simulation results presented in the last two rows of Table 3 of subsection 4.1.1 and experimentally obtained results for the same coils presented in Table 4 of subsection 5.1 can now be compared.

Firstly, theoretical and experimental values of thermal coil performance will be overviewed. Using *COMSOL Multiphysics 5.4*, it was obtained that due to ohmic heating, a 4mm diameter, 0.035mm copper thickness, 0.1mm track width and spacing single-layer flat coil would heat up to a maximum of 58°C when passing 0.5A current through it. Then, on a physical PCB testbed with isolated flat coil of the same parameters, 0.5A current was passed through and the temperature was allowed to settle for 1 minute. A deviation from the theory was observed, with a maximum of 47°C reached. The same was then performed for an identical two-layer coil. With FEM simulation, the result of a maximum of 84°C was reached, while experimentally obtained value matched the theory perfectly, showing 84°C.

The difference obtained for a single-layer coil is non-negligible, with experimental value being nearly 20% lower than the theoretical. This difference might potentially be due to the limited boundary used for FEM simulations, which means that in reality, more heat could be dissipated through the rest of the PCB, as well as to the environment. Moreover, the experimental result for the double-layer coil matched the theory exactly, however, it is potentially due to the fact that experimentally obtained resistance of the double-layer coil is nearly 67% higher than the theoretical value, while for the single-layer coil it is only 33% higher, causing less extra ohmic heating. All in all, these results force the conclusion, that simulations with larger boundary should be performed, as well as extra measurements with higher accuracy multimeter should be obtained.

Next, magnetic flux density results can be overviewed. With FEM simulation software, it was obtained that the single-layer coil should be able to produce a maximum of 7.0mT magnetic flux density, while the double-layer coil should reach a maximum of 7.3mT value. Then, with a *Lakeshore Model 475 DSP* gaussmeter, it was experimentally shown that a single-layer coil can reach a maximum of 0.6mT, while double-layer coil can reach up to 0.9mT. This result is an order of magnitude lower than obtained from FEM simulation, however, as noted in subsection 4.1.1, magnetic flux density for a dipole drops off at a rate of distance cubed. This, in combination with the fact that a hall effect sensor within the probe is at least 0.39mm, at most 1.14mm away from the surface of the coil itself, allows to redefine the theoretically obtained value for the single-layer coil from 7.0mT maximum to a measurable and comparable range of 0.6mT to 1.6mT presented in Fig. 36. Similarly, for the two-layer coil the measurable range was evaluated to be in between 0.8mT and 1.8mT. As can be seen now, the theoretical and experimental values are much closer - even within the same range, albeit on the lower side of it. Nonetheless, due to the small size of the coils, additional

testing setup, and perhaps more suitable measuring equipment, would be needed in order to evaluate the accuracy of FEM results more rigorously.

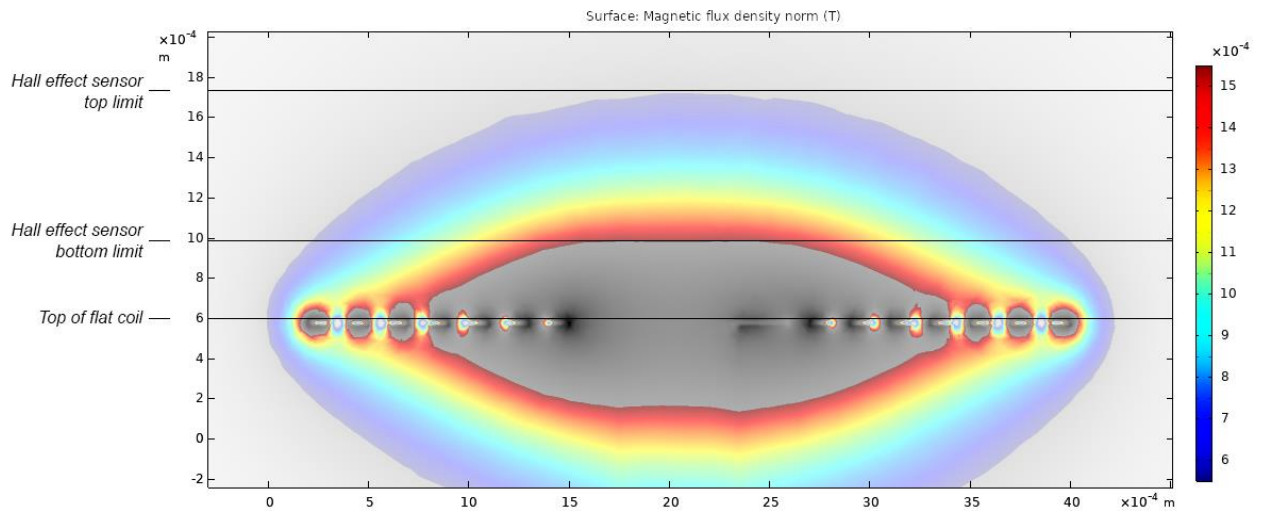


Fig. 36. FEM simulation result of a single-layer coil for magnetic flux density between 0.6mT and 1.6mT

Another important part of the experimental work was determining the payload of the two individual coils. The maximum payload achieved was with the smallest footprint (3mm cube) N42 magnet. It reached a maximum of 1.3g (not considering the mass of the magnet itself) at 1.30A for the single-layer coil, and at 0.69A for the double-layer coil. As the power consumption and heating is proportional to the square of the current, evidently the double-layer coil is more efficient. Nonetheless, at 0.69A it is very close to the determined maximum current allowed before the PCB reaches its limit temperature. Before that, however, when magnet is in direct contact with the PCB, magnet would reach its demagnetization temperature, which is near 70°C. As a result, approximately 1g of continuous payload could be supported by one double-layer coil without causing the magnet to lose its magnetism. Consequently, with the current setup, at least 10 magnets would be needed to provide a continuous 10g payload set out to achieve at the beginning of this work.

However, as with the heating and magnetic flux density, there is potential for improvement of the payload capacity, but further experiments of the PCB-based flat electromagnetic coils would be needed. Firstly, stronger 3mm cube magnet should be obtained and tested, as well as an additional round magnet of 3mm in diameter and 3mm in height. Next, as the smallest footprint magnet performed best, considering that the smaller the PCB-based flat coil is, the more uniform magnetic flux distribution becomes, a smaller diameter flat coils should be tested, with an addition of three-layer coil. Lastly, more options for heat dissipation should be considered, this way allowing for higher payload capacity with the same setup.

Finally, different arrays of coils for linear, rotary and planar motions were implemented and tested. While it was very straightforward to produce basic motion in steps from coil to coil, it is much more complex to generate a code which would produce smooth and easily controllable motion. Generally, for this purpose, motor drivers are implemented, and it would not be an exception in this case. However, the amount of work needed to implement a motor driver is outside of the scope of this project, hence only tests for basic motion to achieve 100mm/s linear speed, 120rpm rotational speed, and demonstrate the potential for planar motion were successfully carried out.

7. Economic Viability of Custom Planar Drive With PCB-Based Stator

In this chapter, a hypothetical scenario of the research subject being made into a sellable product is considered. It is assumed that the development of the first working 6D planar drive with a PCB-based stator coils proposed here is completed, with some ongoing research and development work continuing throughout the year. Furthermore, it is assumed that this is a made-to-order product, built to specifications provided by the customer. The target audience for the custom electromagnetic drive is taken to be mostly universities and R&D companies, with a yearly demand of 20 custom units.

Now, it is important to consider what the final product looks like. For that, one specific design with 40mm-by-40mm active area is considered. Then, a single complete hardware set of such design consists of:

- A PCB-based stator, 50mm by 50mm in size, with a 10 by 10 grid of flat coils.
- Another PCB with control electronics, including *STM32* microprocessor, 5 24-bit serial-to-parallel shift registers, power MOSFETs, position sensors, and some additional unforeseen components.
- Power supply unit.
- A mover (or an end-effector), built to customer requirements.
- An anodized aluminum casing, built to customer requirements.
- Packaging with user manual.

Then, as this is a full mechatronic system, it requires some additional non-hardware components. These include a custom-developed control software, adapted to specific customer requirements, and potential after-sales support and servicing, which translates to an optional yearly technical support subscription.

7.1. Costs

Now, the costs involved in producing and selling a yearly volume of 20 units of custom PCB-based planar electromagnetic drives are analyzed. These include both fixed costs and variable costs, with an additional consideration for a capital investment needed to start the operation [40]. A summary of all costs is presented in Table 5, with a more detailed break-down following below. All figures are rough estimates considering high quality items from well-known suppliers found online.

Table 5. Capital investment related costs, as well as a summary of fixed and variable costs

Long-term asset	Cost
Equipment and tools	2 000€
Software license (<i>SolidWorks Standard 2022</i>)	4 000€
Fixed-cost item (yearly)	
Office space rent (all inclusive)	4 000€
Salary for 3 engineers (software, mechanical, electronics)	90 000€
Equipment depreciation	400€
Other expenses	5 000€
Variable-cost item (to produce 1 unit)	
Materials and components	200€

Analysis of costs involved can be started from the necessary capital investment. Firstly, some tools for prototyping, as well as assembly and maintenance are needed. These include a variety of power tools, some hand tools, as well as a 3D printer for quick prototyping. A rough estimate for the value of tools and equipment needed to start the operation would be 2000€. An additional capital investment would be into the software packages necessary to work on such a product. This could potentially include a *Solidworks* license for mechanical engineering work (nearly 4000€ for a perpetual license), *KiCad* for electronic design (free software suit), and *STM32Cube* for embedded programming (free software suit).

Next, fixed-cost items are considered. Firstly, a private serviced office in a shared offices building is considered, costing from a 100€ per person per month, adding up to approximately 4000€ per year for 3 people [41]. Additionally, a monthly salary will be needed for the 3 engineers working full time on further development and maintenance of the product. In Lithuania, monthly salary before taxes in 2021 averaged 1566€ [42], however, considering that salary in Vilnius is generally higher, as well as qualified professional work is needed, a starting 2500€ cost of one workplace for the employer is considered, totaling 90000€ a year. Furthermore, accounting and potentially legal services will be needed occasionally, which is approximated to cost another 5000€ per year. Finally, equipment depreciation over a 5-year period is considered, whereby all the equipment at the end of 5 years is unusable and has no worth. For a 2000€ worth of tools and equipment, this results in 400€ yearly depreciation.

Lastly, variable costs are considered. This includes only the cost for materials and components to produce one unit of product. Considering two PCBs with components, a power supply, a mover, a case for the stator, and packaging with user manual, the total incurred cost equals to roughly 200€ per unit, however, it is highly depending on quantities produced at a time and the necessary precision.

7.2. Pricing

The primary aim of this part of the economic evaluation is to determine the selling price of the developed system. Previous analysis of capital investment, variable and fixed costs will aid in devising an appropriate pricing for the product. It is done assuming 20 units sold a year, and the resulting bare cost of 1 unit is:

$$VFC_1 = VC_1 + \frac{FC_y}{N_y} = 200 + \frac{99400}{20} = 5170 \text{ €} \quad (4)$$

where VFC_1 – the cost of 1 unit including variable and fixed costs; VC_1 – variable cost for 1 unit; FC_y – fixed cost per 1 year; N_y – number of units sold in a year.

Then, profit margin and the selling price needs to be considered. At this point, only business to business sales are considered, which sets a good profit margin to start with at 30%. This results in the final selling price for a unit:

$$SP_1 = VFC_1 \cdot (1 + PM) = 5170 \cdot (1 + 0.3) = 6721 \text{ €} \quad (5)$$

where SP_1 – selling price per unit; PM – chosen profit margin.

The resulting price's competitiveness in the market is difficult to evaluate, as this is a highly specialized product with no exact equivalents on the market. Furthermore, it is a high-precision, 6D

drive capable of operating in a cleanroom environment, with technical support and maintenance included in this price, which makes it a powerful full-package tool for demanding research work. Also, as the majority of total system cost is not related to materials and components, the price of a single unit could be substantially reduced by selling more units every year. For instance, if the sales went up to 100 units a year, the total cost to produce one unit would go down 5 times, approximately to 1000€. Additionally, if this product would not need further development, 1 mechatronic engineer could support the operation of the business, instead of 3 specialists, bringing the fixed cost down approximately threefold.

One last consideration is a break-even point. This indicates the number of products needed to sell at the set price in order to cover total costs. With all the assumptions made previously, the break-even point is reached after selling:

$$Q = \frac{FC_y}{SP_1 - VC_1} = \frac{99400}{6721 - 200} = 15.24 \text{ units} \quad (6)$$

All in all, the economic evaluation provided in this chapter is based on many assumptions, as it would require more in-depth market analysis to determine more realistic product demand and relevant competitors, as well as potential customers. Nonetheless, it serves as a good starting point to begin evaluating if this could be built into a viable business. Also, it offers some insights into which factors could be addressed first in order to achieve better pricing and reduce overall costs.

Conclusions

1. To begin with, various flat electromagnetic coils were modelled and analyzed using FEM. This has demonstrated that two of the best performing coils were both with 0.1mm track width and spacing, 0.035mm copper layer thickness, and 4mm in diameter, with the only difference being the number of layers. Two-layer flat coil showed a maximum of 7.3mT magnetic flux density at 0.5A current, while reaching a maximum of 84°C temperature. A single-layer coil demonstrated slightly lower magnetic flux density of 7.0mT, however, it has reached only 58°C temperature, which is crucial in keeping stable coil performance without demagnetizing permanent magnets to be used for the actuator's movers. For this reason, single-layer flat coil was chosen as the basis for PCB-based electromagnetic drive's stator.
2. Next, a physical prototype of the two discussed flat coils was developed and evaluated. With thermal imaging camera, it was obtained that a single-layer coil heats up to 47°C when 0.5A current is allowed to flow through it, while a double-layer coil heats up to 84°C. Close to 20% deviation in the obtained heating of a single-layer coil can be attributed to two factors: limited size boundary used for FEM simulations, which if increased, should reduce the theoretical maximum temperature; variable factual resistance of the coils, which explains why only the single-layer coil has difference in obtained maximum temperature.
Now, magnetic flux density obtained experimentally showed 0.6mT for a single-layer coil, and 0.9mT for a double-layer flat coil. This is an order of magnitude lower than maximum theoretically obtained values. However, the equipment used to obtain the experimental values could measure the magnetic flux density from 0.39mm to 1.14mm away from the surface of the coil itself, which explains the large difference. Theoretically, within the said range, single layer coil should achieve between 0.6mT and 1.6mT, and double-layer coil between 0.8mT and 1.8mT. This is in line with experimentally obtained values.
3. Final stage of the project was to design and evaluate a proof-of-concept electromagnetic drive with a PCB-based stator. For this purpose, 3 distinct 16-coil stator configurations were developed: 64mm long single-coil wide strip for linear motion tests with single magnet as a mover; rotary drive using 16 coils distributed around the perimeter of a 30mm diameter circle as a stator, together with 2-magnet symmetrical rotor within 3D printed case; 4-by-4 grid of coils as a stator, together with 4 magnets encased in a 3D printed mover.
4. For all 3 drives, the same electronics setup with similar code for stepping from coil-to-coil was implemented. Maximum achieved linear speed was approximately 101mm/s, while maximum achieved rotational speed was 125rpm. This is by no means a maximum possible speed, as it was accomplished with a very simple stepping algorithm, which limits how smoothly can the drive run, as well as its achievable resolution. In fact, as with any other motor, custom drivers would be required to achieve smooth and easily controllable motion, however, it was outside the scope of this work.

As for the system payload, both single-layer and double-layer coils were evaluated independently. It was obtained that both coils have a maximum payload capacity of approximately 1.5g when used with N42 cube magnet of 3mm per side. For this, single-layer coil required 1.30A of current, while double-layer coil needed 0.69A, which in both cases would result in being very close to the maximum allowable PCB temperature. Therefore, for continuous payload without causing demagnetization to the permanent magnets, approximately 1g continuous maximum payload could be supported.

5. In addition to developing a proof-of-concept PCB-based electromagnetic drive, a hypothetical scenario, where such a drive is brought to the level of a working product was analyzed in order to evaluate its economic viability. The key assumptions made were that 3 full-time engineers (electronic, mechanical and software) are employed in order to maintain and further develop the product to customer specifications, as well as 20-unit demand of custom drives a year is present. Under these circumstances, one unit needs to be sold for 6721€, considering a 30% profit margin. The final price, however, is highly dependent on the assumptions made, meaning that the price could be 3 to 5 times lower if the yearly demand reached 100 units, or 1 mechatronic engineer instead of 3 specialist engineers were working on maintaining and developing the product.

List of references

1. ZHU, Haiyue, PANG, Chee Khiang and TEO, Tat Joo. Analysis and control of a 6 DOF maglev positioning system with characteristics of end-effects and eddy current damping. *Mechatronics*. 1 November 2017. Vol. 47, p. 183–194. DOI 10.1016/j.mechatronics.2016.12.004.
2. DYCK, M., LU, X. and ALTINTAS, Y. Magnetically Levitated Rotary Table With Six Degrees of Freedom. *IEEE/ASME Transactions on Mechatronics*. February 2017. Vol. 22, no. 1, p. 530–540. DOI 10.1109/TMECH.2016.2621108.
3. LIU, Yan and RAVINDRA, Nuggehalli M. A Magnetic-Field-Assisted Milli-Scale Robotic Assembly Machine: An Approach to Parallel Robotic Automation Systems. *Micromachines*. 23 March 2018. Vol. 9, no. 4, p. 144. DOI 10.3390/mi9040144.
4. HSU, Allen, ZHAO, Huihua, GAUDREAU, Martin, FOY, Annjoe Wong and PELRINE, Ron. Magnetic Milli-Robot Swarm Platform: A Safety Barrier Certificate Enabled, Low-Cost Test Bed. *IEEE Robotics and Automation Letters*. April 2020. Vol. 5, no. 2, p. 2913–2920. DOI 10.1109/LRA.2020.2974713.
5. SALIM, Neethu, NIKAM, Saurabh Prakash, PAL, Saumitra, WANKHEDE, Ashok Krishnrao and FERNANDES, Baylon Godfrey. Multiphysics analysis of printed circuit board winding for high-speed axial flux permanent magnet motor. *IET Electric Power Applications*. 2019. Vol. 13, no. 6, p. 805–811. DOI 10.1049/iet-epa.2018.5752.
6. MARIGNETTI, Fabrizio, VOLPE, Giuseppe, MIRIMANI, Seyyed Mehdi and CECATI, Carlo. Electromagnetic Design and Modeling of a Two-Phase Axial-Flux Printed Circuit Board Motor. *IEEE Transactions on Industrial Electronics*. January 2018. Vol. 65, no. 1, p. 67–76. DOI 10.1109/TIE.2017.2716865.
7. ZHU, Haiyue, TEO, Tat Joo and PANG, Chee Khiang. Design and Modeling of a Six-Degree-of-Freedom Magnetically Levitated Positioner Using Square Coils and 1-D Halbach Arrays. *IEEE Transactions on Industrial Electronics*. January 2017. Vol. 64, no. 1, p. 440–450. DOI 10.1109/TIE.2016.2598811.
8. Magnetic levitation stage with planar motor. *Philips Engineering Solutions* [online]. [Accessed 28 February 2022]. Available from: <https://www.engineeringsolutions.philips.com/news/magnetic-levitation-stage-planar-motor/>
9. TAQAVI, Omolbanin and MIRIMANI, Seyed Mehdi. Design aspects, winding arrangements and applications of printed circuit board motors: a comprehensive review. *IET Electric Power Applications*. 2020. Vol. 14, no. 9, p. 1505–1518. DOI 10.1049/iet-epa.2020.0141.
10. HUNTER, Elizabeth E., STEAGER, Edward B., HSU, Allen, WONG-FOY, Annjoe, PELRINE, Ron and KUMAR, Vijay. Nanoliter Fluid Handling for Microbiology Via Levitated Magnetic Microrobots. *IEEE Robotics and Automation Letters*. April 2019. Vol. 4, no. 2, p. 997–1004. DOI 10.1109/LRA.2019.2893682.
11. HSU, Allen, COWAN, Cregg, CHU, William, MCCOY, Brian, WONG-FOY, Annjoe, PELRINE, Ron, VELEZ, Camilo, ARNOLD, David, LAKE, Joseph, BALLARD, Joshua and RANDALL, John. Automated 2D micro-assembly using diamagnetically levitated milli-robots. In : *2017 International Conference on Manipulation, Automation and Robotics at Small Scales (MARSS)*. July 2017. p. 1–6.

12. PELRINE, Ron, HSU, Allen, COWAN, Cregg and WONG-FOY, Annjoe. Multi-agent systems using diamagnetic micro manipulation — From floating swarms to mobile sensors. In : *2017 International Conference on Manipulation, Automation and Robotics at Small Scales (MARSS)*. July 2017. p. 1–6.
13. PAWINANTO, Roer, YUNAS, Jumril, MAJLIS, Burhanuddin and HAMZAH, Azlan. Design and Fabrication of Compact MEMS Electromagnetic Micro-Actuator with Planar Micro-Coil Based on PCB. *TELKOMNIKA (Telecommunication Computing Electronics and Control)*. 1 September 2016. Vol. 14, p. 856. DOI 10.12928/telkomnika.v14i3.3998.
14. UEDA, Y. and OHSAKI, H. A Long-Stroke Planar Actuator with Multiple Degrees of Freedom by Minimum Number of Polyphase Currents. In : . 2010.
15. ROVERS, J.M.M., JANSEN, J.W. and LOMONOVA, E.A. Design and measurements of the Double Layer Planar Motor. In : *2013 International Electric Machines Drives Conference*. May 2013. p. 204–211.
16. SCHÄFFEL, Christoph, KATZSCHMANN, Michael, MOHR, Hans-Ulrich, GLOESS, Rainer, RUDOLF, Christian, MOCK, Christopher and WALENDA, Carolin. 6D planar magnetic levitation system - PIMag 6D. *Mechanical Engineering Journal*. 16 October 2015. DOI 10.1299/mej.15-00111.
17. LU, Xiaodong and USMAN, Irfan-ur-rab. 6D direct-drive technology for planar motion stages. *CIRP Annals*. 1 January 2012. Vol. 61, no. 1, p. 359–362. DOI 10.1016/j.cirp.2012.03.145.
18. GLOESS, Rainer and GOOS, Alexander. Magnetic levitation stages for planar and linear scan application with nanometer resolution. *International Journal of Applied Electromagnetics and Mechanics*. 1 January 2020. Vol. 63, no. 1, p. 105–117. DOI 10.3233/JAE-209003.
19. ROVERS, J.M.M., JANSEN, J.W. and LOMONOVA, E.A. Design and measurements of the Double Layer Planar Motor. In : *2013 International Electric Machines Drives Conference*. May 2013. p. 204–211.
20. ROVERS, J. M. M., JANSEN, J. W. and LOMONOVA, E. A. Multiphysical analysis of moving-magnet planar motor topologies. *IEEE Transactions on Magnetics*. December 2013. Vol. 49, no. 12, p. 5730–5741. DOI 10.1109/TMAG.2013.2273060.
21. LIU, F., ZHANG, M., ZHU, Y. and HU, C. A Real-Time Model of Ironless Planar Motors With Stationary Circular Coils. *IEEE Transactions on Magnetics*. July 2015. Vol. 51, no. 7, p. 1–10. DOI 10.1109/TMAG.2015.2397873.
22. NGUYEN, Vu Huy and KIM, Won-jong. Two-Phase Lorentz Coils and Linear Halbach Array for Multiaxis Precision-Positioning Stages With Magnetic Levitation. *IEEE/ASME Transactions on Mechatronics*. December 2017. Vol. 22, no. 6, p. 2662–2672. DOI 10.1109/TMECH.2017.2769160.
23. What is a Printed Circuit Board (PCB)? | Its Structure And Types. [online]. [Accessed 13 November 2021]. Available from: <https://www.pcbonline.com/blog/what-is-printed-circuit-board.html>
24. What Affect PCB Assembly Cost? [online]. [Accessed 13 November 2021]. Available from: <https://www.jycircuitboard.com/news/what-affect-pcb-assembly-cost--282.html>

25. PCB Prototype & PCB Fabrication Manufacturer - JLCPCB. [online]. [Accessed 9 January 2022]. Available from: <https://jlcpcb.com/capabilities>
26. PCB Capabilities - Custom PCB Prototype the Easy Way - PCBWay. [online]. [Accessed 9 January 2022]. Available from: <https://www.pcbway.com/capabilities.html>
27. Eurocircuits - Eurocircuits Eurocircuits Eurocircuits. *Eurocircuits* [online]. [Accessed 9 January 2022]. Available from: <https://www.eurocircuits.com/technical-specifications-of-all-eurocircuits-prototype-small-volume-services-european-origin/>
28. PAWINANTO, Roer, YUNAS, Jumril, SAID, Muzalifah, MOHD NOOR, Mimiwyat and MAJLIS, Burhanuddin. Design and Fabrication of PCB Based Planar Micro-coil For Magnetic MEMS Actuator. In : *IEEE International Conference on Semiconductor Electronics, Proceedings, ICSE*. 29 August 2014.
29. PAWINANTO, Roer, YUNAS, Jumril, MAJLIS, Burhanuddin and HAMZAH, Azlan. Design and Fabrication of Compact MEMS Electromagnetic Micro-Actuator with Planar Micro-Coil Based on PCB. *TELKOMNIKA (Telecommunication Computing Electronics and Control)*. 1 September 2016. Vol. 14, p. 856. DOI 10.12928/telkomnika.v14i3.3998.
30. MORETON, Gregory, MEYDAN, Turgut and WILLIAMS, Paul. Using finite element modelling and experimental methods to investigate planar coil sensor topologies for inductive measurement of displacement. *AIP Advances*. 1 April 2018. Vol. 8, no. 4, p. 047503. DOI 10.1063/1.4994127.
31. Carl Bugeja - YouTube. [online]. [Accessed 14 November 2021]. Available from: <https://www.youtube.com/c/CarlBugeja/featured>
32. STM32F103C8T6 - Blue Pill Development Board. *Components101* [online]. [Accessed 24 April 2022]. Available from: <https://components101.com/microcontrollers/stm32f103c8t8-blue-pill-development-board>
33. *1912230.pdf* [online]. [Accessed 24 April 2022]. Available from: <https://www.farnell.com/datasheets/1912230.pdf>
34. Proster VC99 | Test Meter PRO. [online]. [Accessed 23 April 2022]. Available from: <http://testmeterpro.com/proster-vc99/>
35. Seek Shot Series - Powerful Pocket-Sized Thermal Imaging. *Seek Thermal | Affordable Infrared Thermal Imaging Cameras* [online]. [Accessed 23 April 2022]. Available from: <https://www.thermal.com/seekshot-series.html>
36. Model 475 DSP Gaussmeter. *Default* [online]. [Accessed 23 April 2022]. Available from: <https://www.lakeshore.com/products/categories/overview/magnetic-products/gaussmeters-teslameters/model-475-dsp-gaussmeter>
37. Precision laboratory power supply LongWei PS3010DF 0-30V 10A. *Precision laboratory power supply LongWei PS3010DF 0-30V 10A* [online]. [Accessed 23 April 2022]. Available from: <https://www.anodas.lt/en/precision-laboratory-power-supply-longwei-ps3010df-0-30v-10a>
38. TMC2209 Stepper Motor Driver Module. *Components101* [online]. [Accessed 26 April 2022]. Available from: <https://components101.com/modules/tmc2209-stepper-motor-driver-module>

39. BUDIMIR, Miles. Microstepping myths. *Machine Design* [online]. 9 October 2003. [Accessed 27 April 2022]. Available from: <https://www.machinedesign.com/archive/article/21812154/microstepping-myths>
40. Variable Costs. *Corporate Finance Institute* [online]. [Accessed 8 May 2022]. Available from: <https://corporatefinanceinstitute.com/resources/knowledge/accounting/variable-costs/>
41. Office Space for Rent in Lithuania | Serviced Office | Regus. [online]. [Accessed 8 May 2022]. Available from: <https://www.regus.com/en-us/lithuania>
42. BNS, Agnė Vareikaitė-Mills. Vidutinis paskaičiuotas atlyginimas per metus padidėjo 12%, per ketvirtį – 3,2%. *vz.lt* [online]. [Accessed 8 May 2022]. Available from: <https://www.vz.lt/verslo-valdymas/2021/08/27/vidutinis-paskaiciuotas-atlyginimas-per-metus-padidejo-12-per-ketvirti--32>